Ground Magnetometer, VLF-EM and EM-31MK2 Surveys – Olympian Gold Project Triggs Mine Area Grid April 7 to 13, 2010

Report for:
Nuinsco Resources Ltd.
1802-80 Richmond St W.
Toronto ON
M5H 2A4

John G. Hayles P.Eng.
Geophysicist
Hayles Geoscience Surveys Ltd.
511 Robinson Avenue
Selkirk, Manitoba
R1A 1E5
www.haylesgeoscience.ca

July 14, 2010

Table of Contents

List of Figures

Introduction

A ground geophysical survey was completed from April 6 to 13, 2010 on a grid surrounding the former Triggs Mine south east of Kenora, Ontario (see Figures 1,2 and 3). This work was done for C.A. Wagg P.Geo on behalf of Nuinsco Resources Limited. About 1890 measurements were recorded at about 12.5-m intervals on approximately 23.7-km of grid line with a ground magnetometer and VLF-EM system linked to a real-time differentially corrected GPS. In addition, an EM-31MK2 scan was completed of the showing area on April 12 and four detail EM-31 profiles were recorded on April 13. This report describes the survey, results and discusses interpretation.

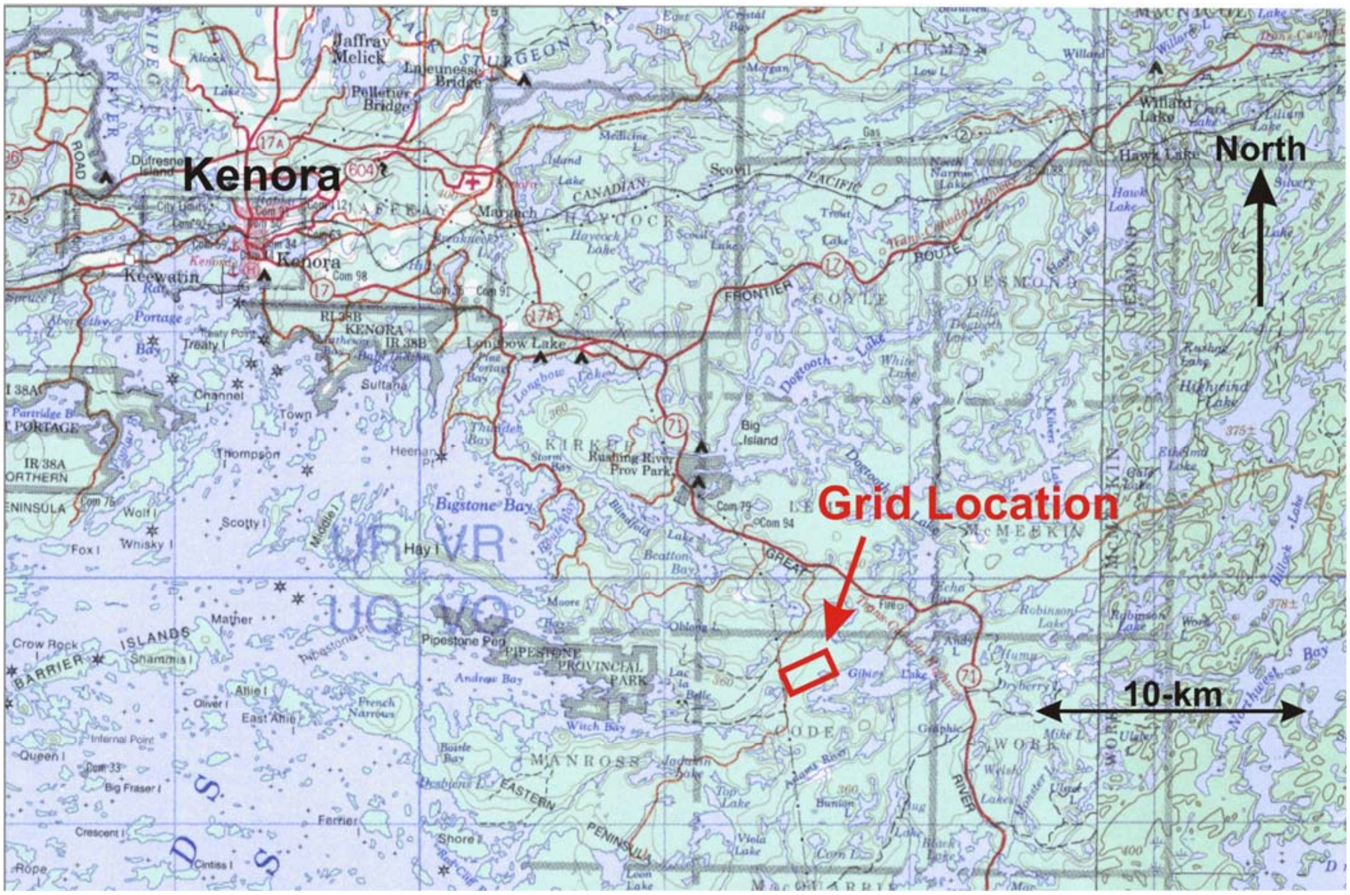

Figure 1. The survey grid is centred on the former Triggs Mine about 40-km south-east of Kenora, Ontario.

Site Description

The survey grid, as designed, is shown in Figure 2 superimposed on an air-photograph. Access is about 20-minutes along the gravel base Witch Bay road from Highway 71. The grid consist of about 2000-m of baseline and 21,225-m of cross-line. The lines were labelled from 0-West to 20-W.

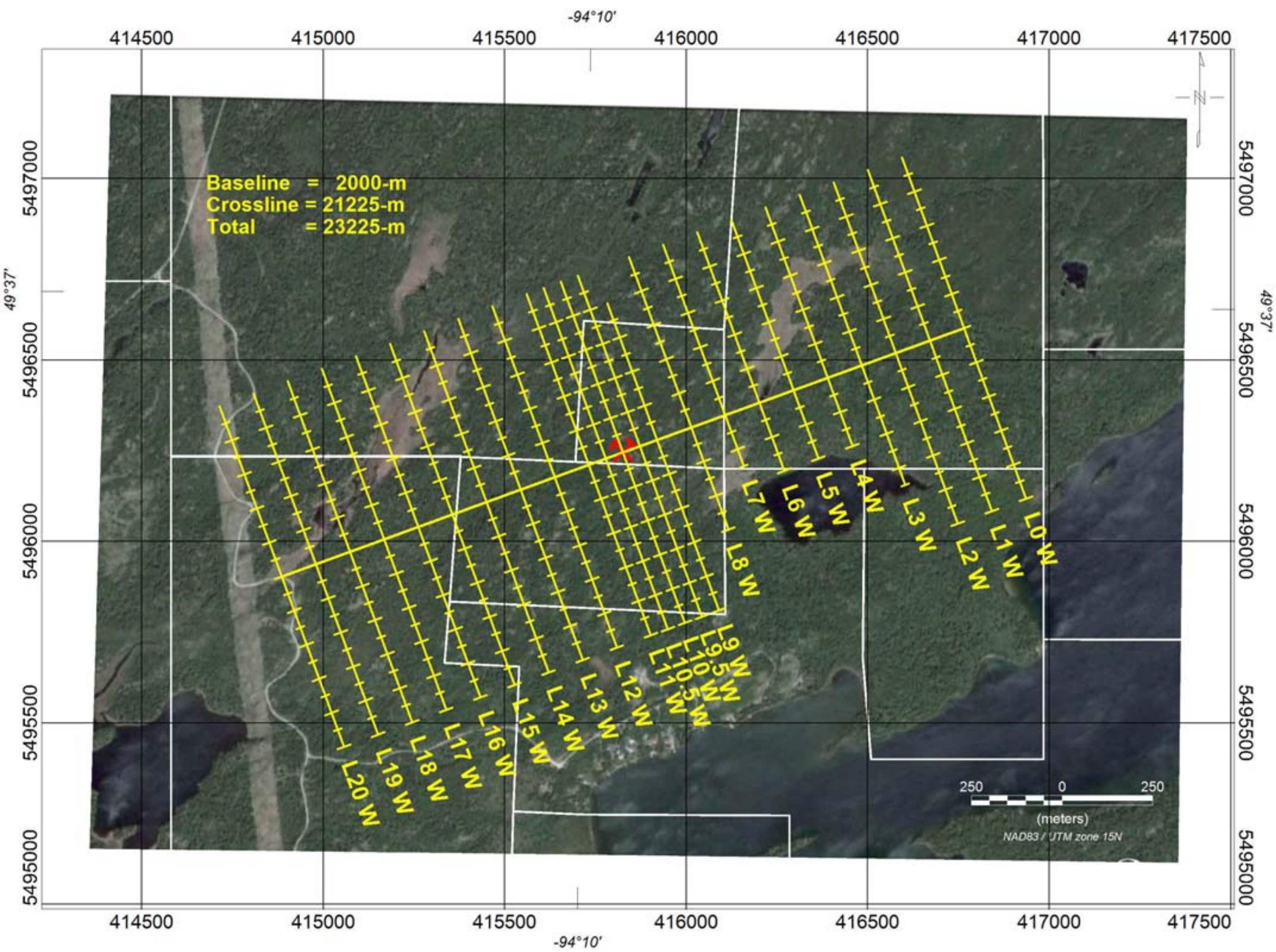

Figure 2. The approximate grid location is superimposed on an air-photograph of the area. Claim lines, as defined by the provincial government on-line database, are shown in white.

A map of the former Triggs Mine showing area is shown in Figure 3 below. There are several trenches and small buildings.

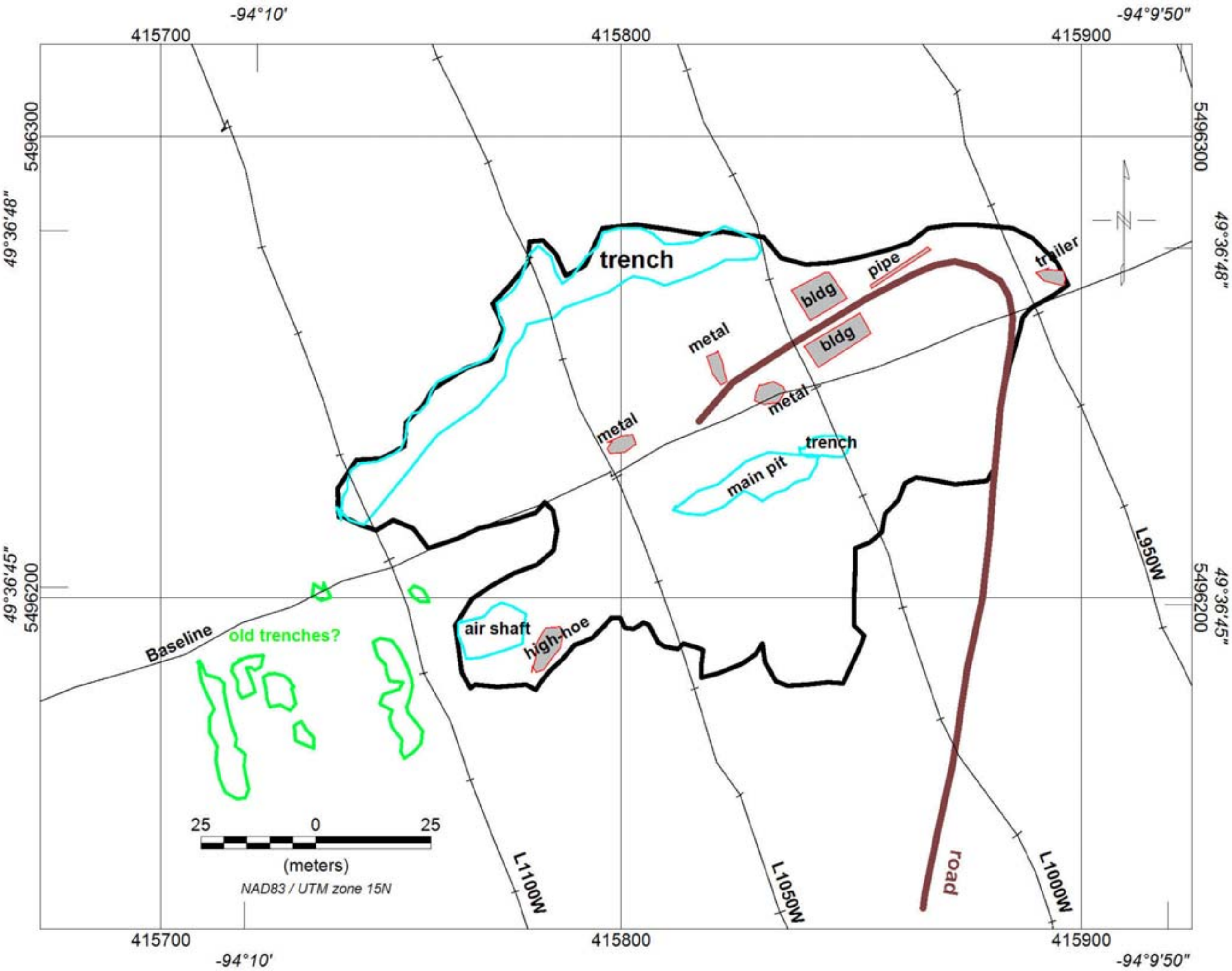

Figure 3. A map of the central showing of the former Triggs Mine is shown here.

Instruments and Methods

The measurements on the main grid were made with a GEM Systems Inc GSM-19 rover magnetometer (serial number 8032671) with VLF-EM and CDGPS measurement capabilities. A second GSM-19 magnetometer (serial number 6011780) was used as a base station to record diurnal variations of the earth's magnetic field during the survey. Both magnetometers are Overhauser-type with an absolute accuracy of about ± 0.1-nT. The rover magnetometer was used in line-and-station mode with 12.5-m between measurements along the lines.

Real-time differentially corrected UTM coordinates were recorded simultaneously with the magnetometer and VLF-EM measurements at ~12.5-m spacing along the survey lines. This real-time GPS uses the Canadian Differential corrections network and has a horizontal accuracy of about ± 0.5-m and a vertical uncertainty of ±1.5-m.

In addition to the GSM-19 GPS, a Trimble Pro-XRT DGPS system (serial numbers: SS22A14030 data-logger, 4923K62343 receiver, 1440918369 antenna) was used to define claim-lines, claim-posts, clearings, metal objects, trenches and showings. This is a state-of-the-art DGPS with Omni-Star real-time differential correction subscription and a horizontal accuracy of about ±0.3-m.

Figure 4. Photograph of the Gem Systems GSM-19mag/vlf/cdgps system at 12.5m S on Line 1050W.

Figure 5. Photograph of Robert Hood operating the Trimble Pro-XRT DGPS system on site.

The survey personnel were:

Robert Hood	survey assistant, Selkirk, Manitoba
John Hayles	geophysicist, Selkirk, Manitoba

An Operator's Report describing the day-to-day activity for this work has been completed (Hayles 2010). Standard practices were used for the surveys. The base station magnetometer was set up just south of the survey grid (see location in Figure 1). The base station recorded the earth's field every 30-s of each survey day. The rover magnetometer operator removed all iron and/or magnetic objects from his clothing that might interfere with the magnetic field measurements. Watches, belt buckles, steel fasteners, steel-toed boots, baseball hats, metal-rim glasses etc. were not worn during the survey.

The VLF-EM survey recorded signals from NAA (24.0-kHz) in Cutler, Maine and NML (25.2-kHz) in La Moure, North Dakota. VLF-EM for geological exploration is a well known method (McNeill & Labson 1991) and is commonly used in the early stages of a geological characterization program for remote areas. The signals propagate deep in the earth and can help in understanding subsurface fractures, faults and contacts between rock types.

The VLF exploration user community is small and sometimes there are gaps of several years where changes to the VLF transmitters are not common knowledge. The dismantling of VLF station NSS (transmitting at 21.4-kHz) in 1999, the transfer of this frequency to NPM in Hawaii, the arrival of the new 500 kW VLF transmitter station NML (25.2-kHz) in La Moure, North Dakota are some recent developments. Interference between NML and NLK, only 400-Hz apart, is strong in the Triggs area.

The TEC survey was recorded with a Geonics Ltd. EM-31MK2 (serial number: 9929010) (see Figure 6). This instrument measures the apparent electrical conductivity of the earth in **milliSiemens/metre** (mS/m). The **Siemen** is the SI unit of measurement for volume electrical conductance and is equivalent to an **Ampere/Volt**. The Siemen is equivalent to the **mho,** used in the past, and familiar to some readers. The reciprocal of the electrical conductivity is termed the **electrical resistivity**, which has SI unit of **Ohm-metre.** Some earth science specialists prefer to use ohm-metres instead of milliSiemens/metre or Siemens/metre.

A transmitter antenna contained in the EM-31 instrument, sets up a primary electromagnetic (EM) field that causes eddy currents in the earth. These eddy currents create a secondary EM field that has a characteristic intensity and time variation with respect to the primary EM field that is directly related to the electrical conductivity of the earth. A nearby receiver antenna is used to measure the in-phase **in parts per thousand** (*ppt*) of the transmitted field and quadrature (or out-of-phase) components of the resultant electromagnetic field and derives the apparent electrical conductivity from the quadrature component for the earth directly below the instrument. As long as there are no metallic objects nearby and the instrument is over typical soils the measurement of apparent electrical conductivity will be accurate. The spacing between the antenna coils influences the maximum depth of investigation and target resolution varies inversely with depth. Readers interested in the physical principles of the measurement can refer to texts on the subject by Grant and West (1965), Telford (1993), Beck (1991) and Reynolds (1997). McNeill (1980) gives an excellent description of the instrumentation, measurement, and average electrical conductivities of rocks and soils. The EM-31 has depth of inspection of about 3 to 4-m. Smaller (EM-38) and larger scale (EM-34) versions of this instrument also exist.

Figure 6. The EM-31MK2 and DGPS system are shown in operation above.

The EM-31MK2 survey was recorded in walking-mode on April 12 (see Figure 7) with the instrument in the standard vertical magnetic dipole (VMD) orientation with a Trimble TSC2 DGPS receiver mounted on a backpack and logging the EM-31 measurements along with the GPS positions (see Figure 2). About 4900 detail EM-31MK2 measurements were recorded over the showing area in vertical magnetic dipole mode on about 3-km of traverse in April 12.

On April 13, the EM-31MK2 was used in vertical magnetic dipole mode (VMD) and horizontal magnetic dipole (HMD) mode for in-line and cross-line antenna orientation along four detail profiles in the central showing area (see Figure 7).

Table 1 below shows the approximate range of apparent electrical conductivities of near-surface soils and rock in Southern Manitoba. The apparent electrical conductivities for soils and rock in and around this site are probably very similar to those observed in southern Manitoba.

Table 1: Apparent Electrical Conductivities of Soils in Manitoba

Soil Type	Range in Electrical Conductivity*1 (milliSiemens/m)	Typical Values*2 (milliSiemens/m)
Clay	50-200	90 – 120
Silt	30-130	40 – 80
Sand	5-80	10 – 40
Gravel	2-80	5 – 30
Wet & fractured bedrock	2-10	5
Dry unfractured bedrock	<1	1
Sea water	1000 – 3000	

*1. The state of water saturation, pore water salinity, and temperature are the main controls.
*2. Typical values for undisturbed soils in Southern Manitoba.

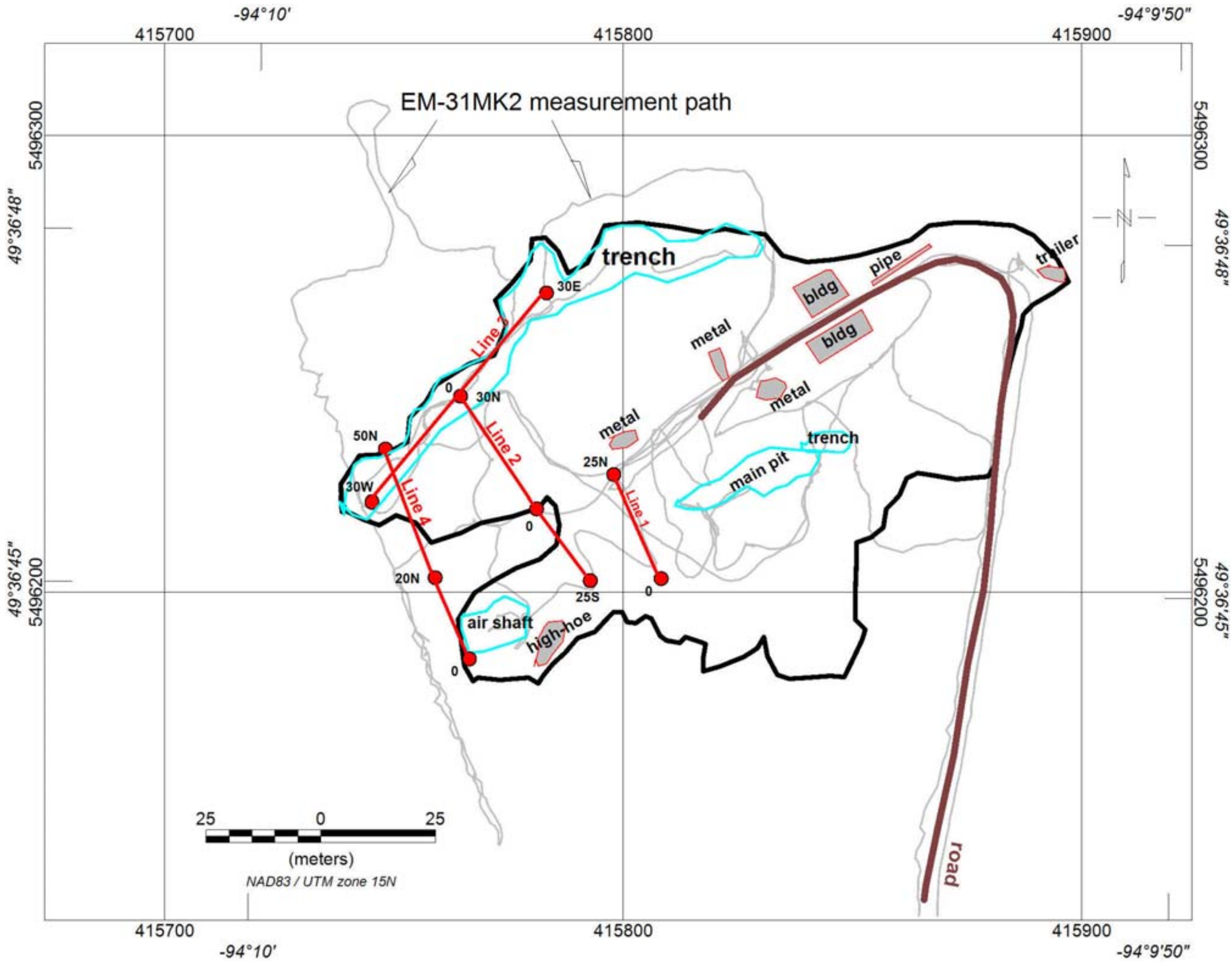

Figure 7. An EM-31MK2 scan was recorded along an irregular track over the main showing area on April 12, 2010. Four detail EM-31 profiles were also collected along Lines 1, 2, 3, and 4 shown above in red on April 13.

Data Reduction and Processing

Standard techniques were used to process and plot the data. At the end of each day the magnetic and VLF data were downloaded to a laptop computer and stored as ASCII files. Base station drift corrections were then applied to the rover data assuming a datum of 58000-nT for the survey area.

Digital copies of the data sets, figures, and maps in this report will be supplied separately on CD archive.

Data Presentation

In addition to the 29 figures in this report, nine plates plotted on ANSI E size (34” by 44”) paper of the geophysical results on the main grid are included at 1:2,500 scale.

Plate 1: Post Plot - Residual Magnetic Field Strength Values
Plate 2: Colour Contour Plot - Residual Magnetic Field Strength
Plate 3: Post Plot - VLF-EM Tilt-Angle and Quadrature Response - NAA
Plate 4: Post Plot - VLF-EM Tilt-Angle and Quadrature Response - NML
Plate 5: Profile Plot - VLF-EM Tilt-Angle and Quadrature Response – NAA
Plate 6: Profile Plot - VLF-EM Tilt-Angle and Quadrature Response – NML
Plate 7: Fraser Filter of the NAA Tilt-Angle Response
Plate 8: Fraser Filter of the NML Tilt-Angle Response
Plate 9: CDGPS Elevation

A CD with the electronic document versions of this report and the eight plates in Adobe Acrobat .PDF format is also included with this report.

Results

About 1890 magnetic and VLF-EM measurements were collected on approximately 23.7-km of line. Table A-1 in the appendix lists the survey production for each day.

Figure 8 below shows an example of repeatability for the magnetometer measurements. Diurnal magnetic field variations have been corrected for in this plot. On April 7, Line 1050W was read from 500S to the baseline every 12.5-m, and then on April 10 this same line was read from the baseline south to 500S. It is difficult for the operator to put the magnetic field sensor in exactly the same location in this type of repeatability demonstration. There are some very strong magnetic fields along this line (> 8000-nT) and in strong fields like this it is important to re-position the sensor within centimetres to millimetres to properly show measurement repeatability. We did not attempt to reposition the sensor to this accuracy for the reconnaissance surveys requested. These strong magnetic fields indicate significant concentrations of magnetite in the shallow subsurface.

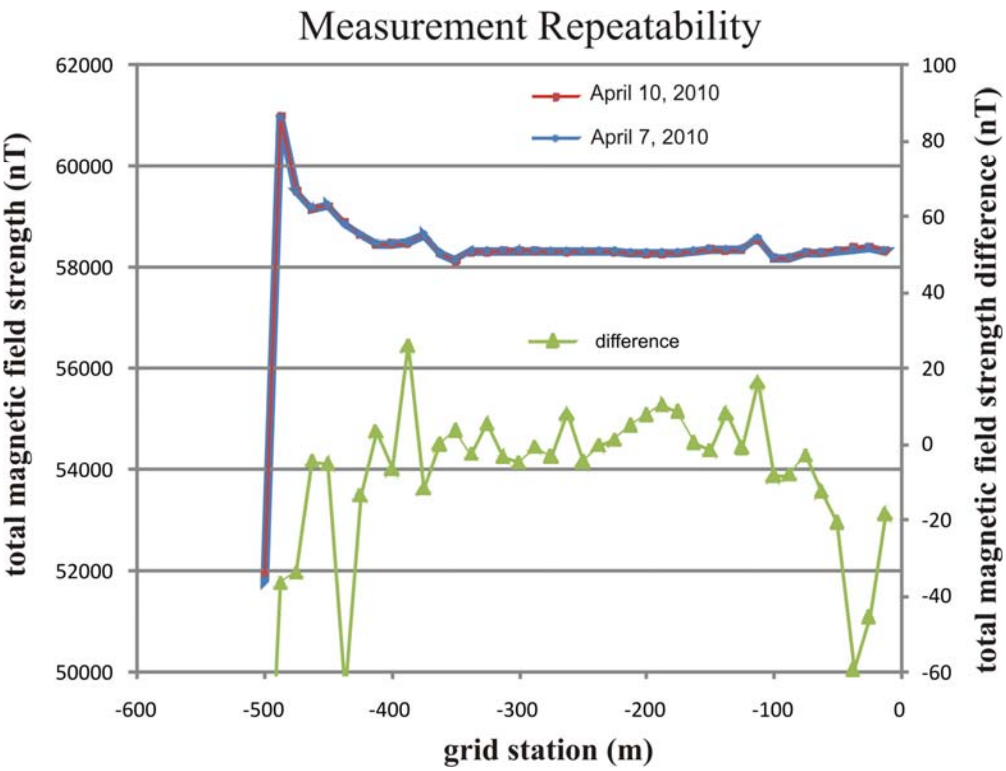

Figure 8. The measurement repeatability for the total magnetic field is shown above for the southern half of Line 1050W which was first recorded April 7 and repeated on April 10.

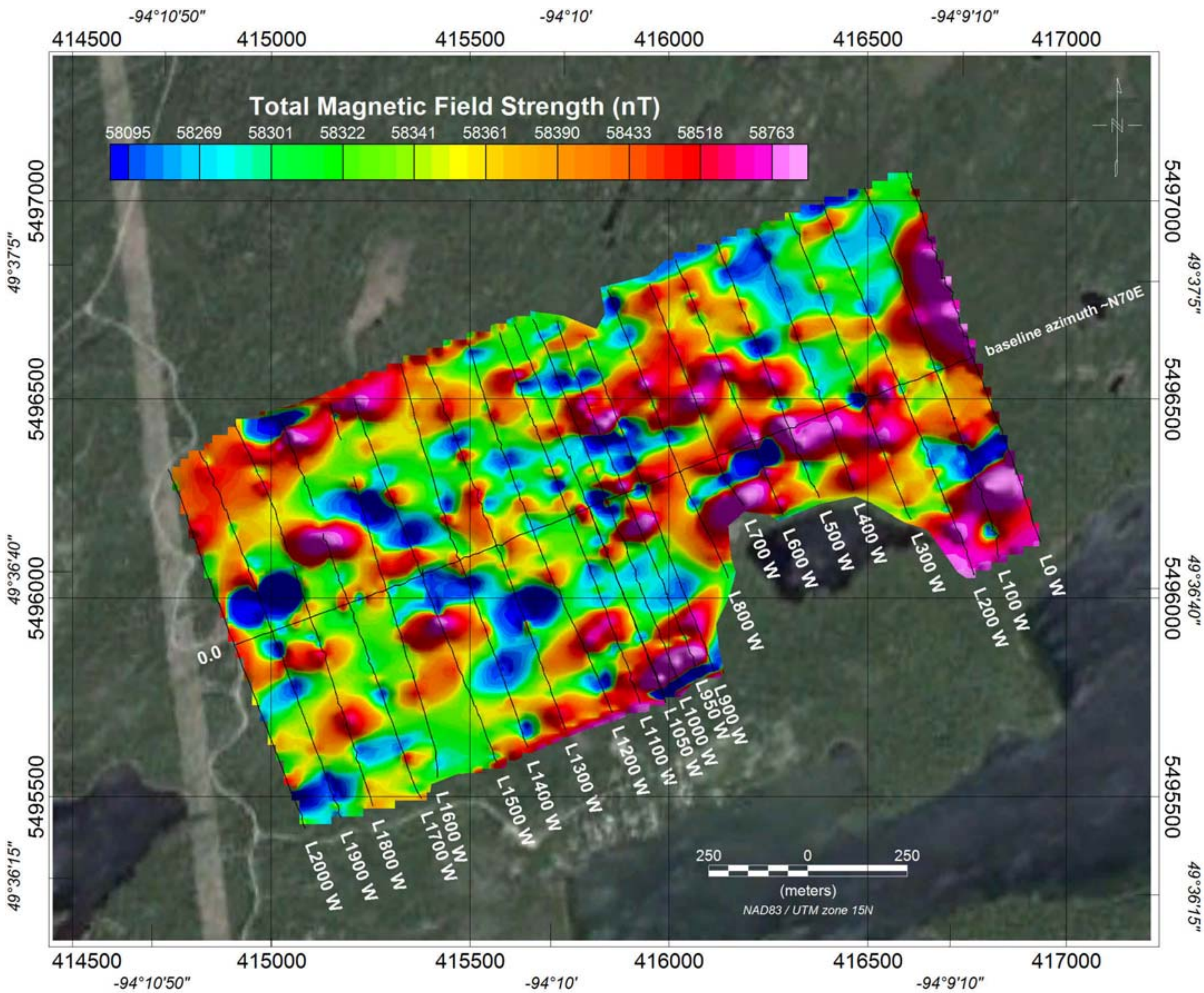

Figure 9. A colour image of the total magnetic field strength over the grid is presented above. There are very strong magnetic fields on this property and there must be significant concentrations of magnetite here. Metal objects may influence some measurements in the former mine workings area.

The magnetic field averages about 58,390-nT ± 500-nT. The maximum value recorded was about 62,400-nT and the minimum value was about 51,800-nT. Figure 10 below presents the areas where the magnetic field measurement signal quality was less that 99%.

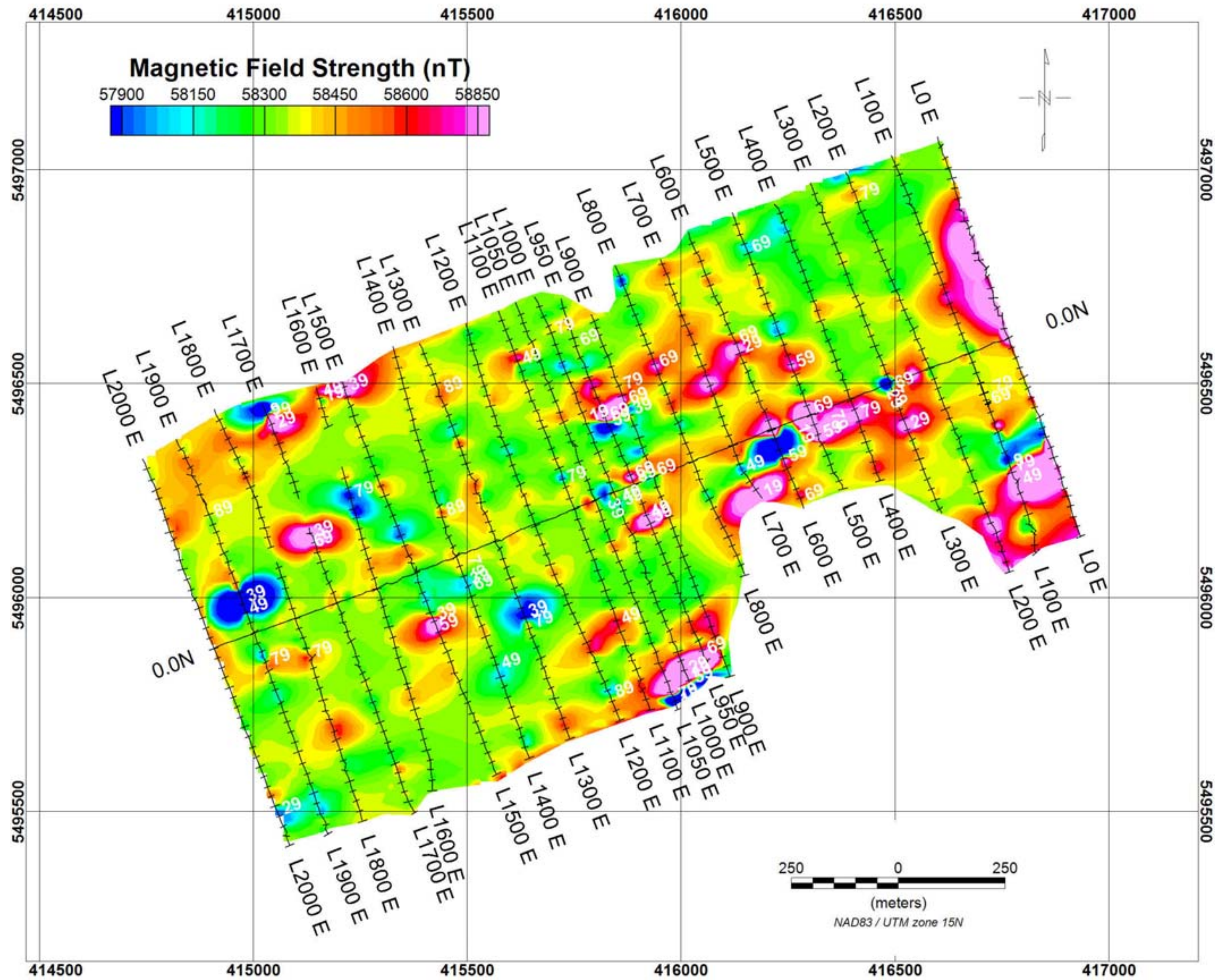

Figure 10. Lower signal-quality measurements for the magnetic field are shown here in white.

Lower signal quality in the magnetic field often indicates a strong magnetic field gradient across the magnetic sensor. The signal quality then gives an idea of how variable the local field is across the sensor. These strong gradients suggest bands of 50% to 100% magnetite near surface.

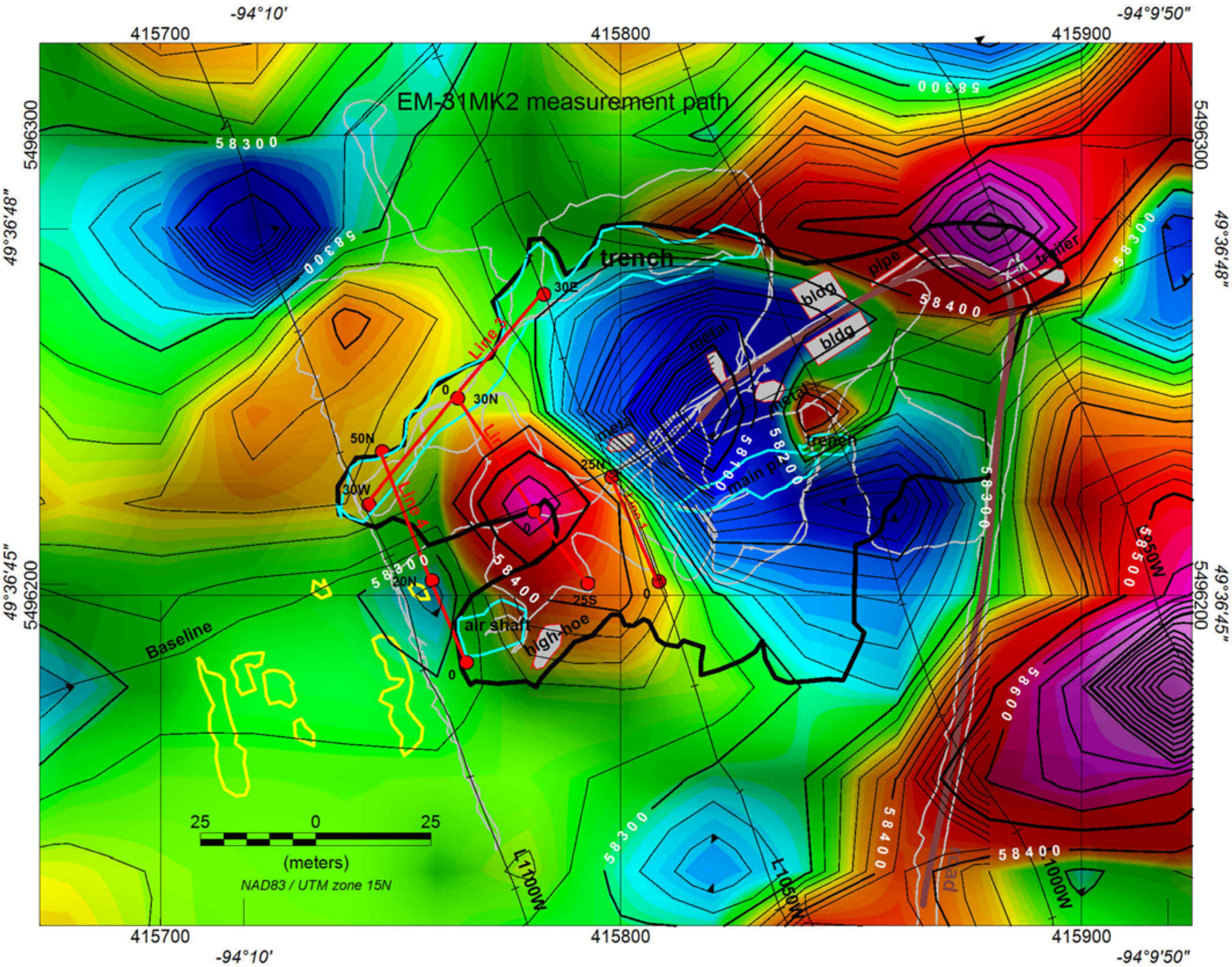

Figure 11. The magnetic field for the detail area around the former Triggs Mine is shown above.

Metal objects are common in the showing area and this makes understanding the geologic patterns in the magnetic field more difficult to recognize. The main low along the baseline between Line 1050W and Line 1000W is probably moderately influenced by manmade iron-bearing objects nearby. The other low at about 60N on Line 1100W may also be steel related.

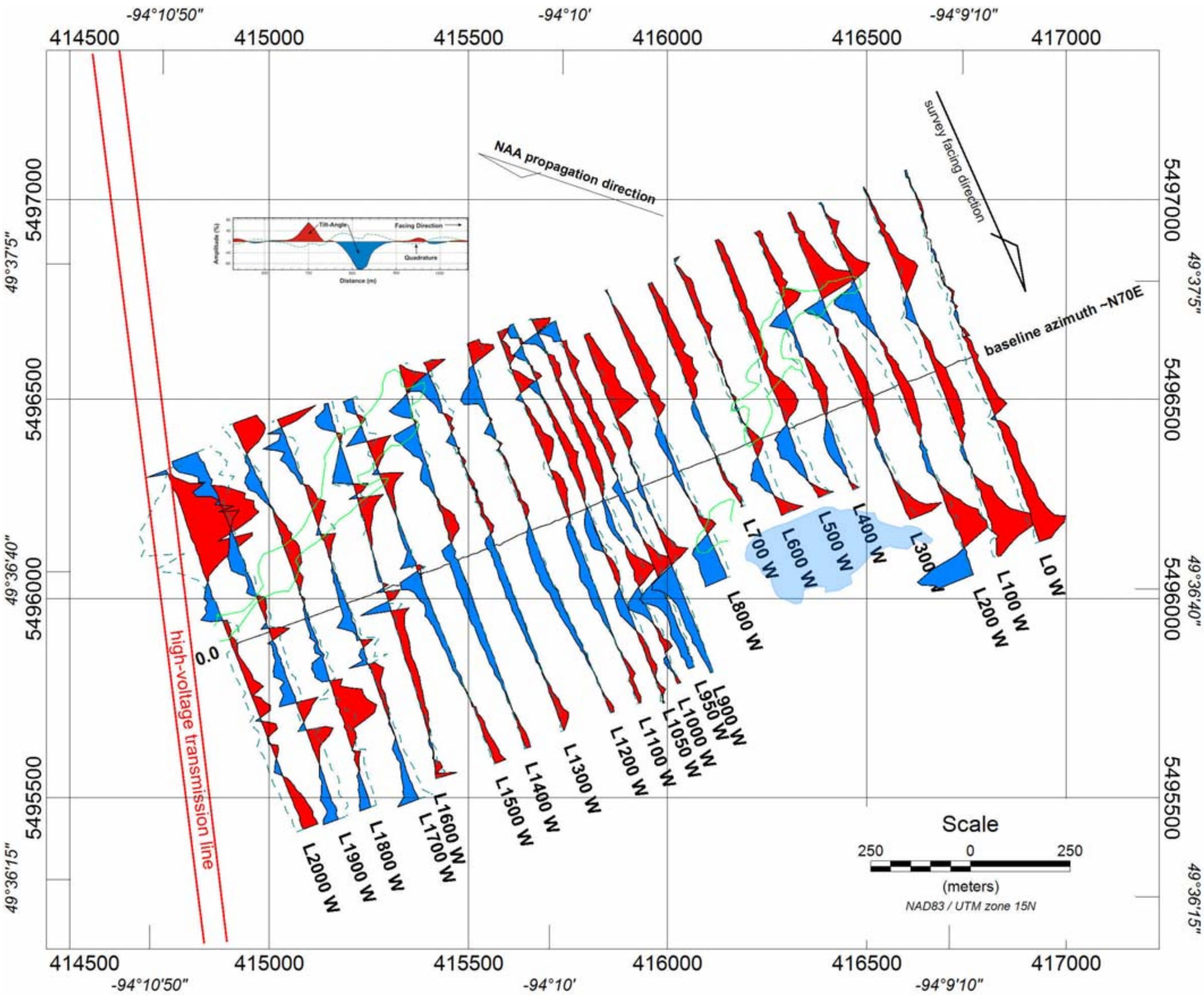

Figure 12. Profiles of the NAA tilt-angle and quadrature response are shown here. The survey facing direction is to the south in this plot.

The large NAA tilt-angle response at the north end of Line 2000W is probably caused by interference from the high-voltage transmission line.

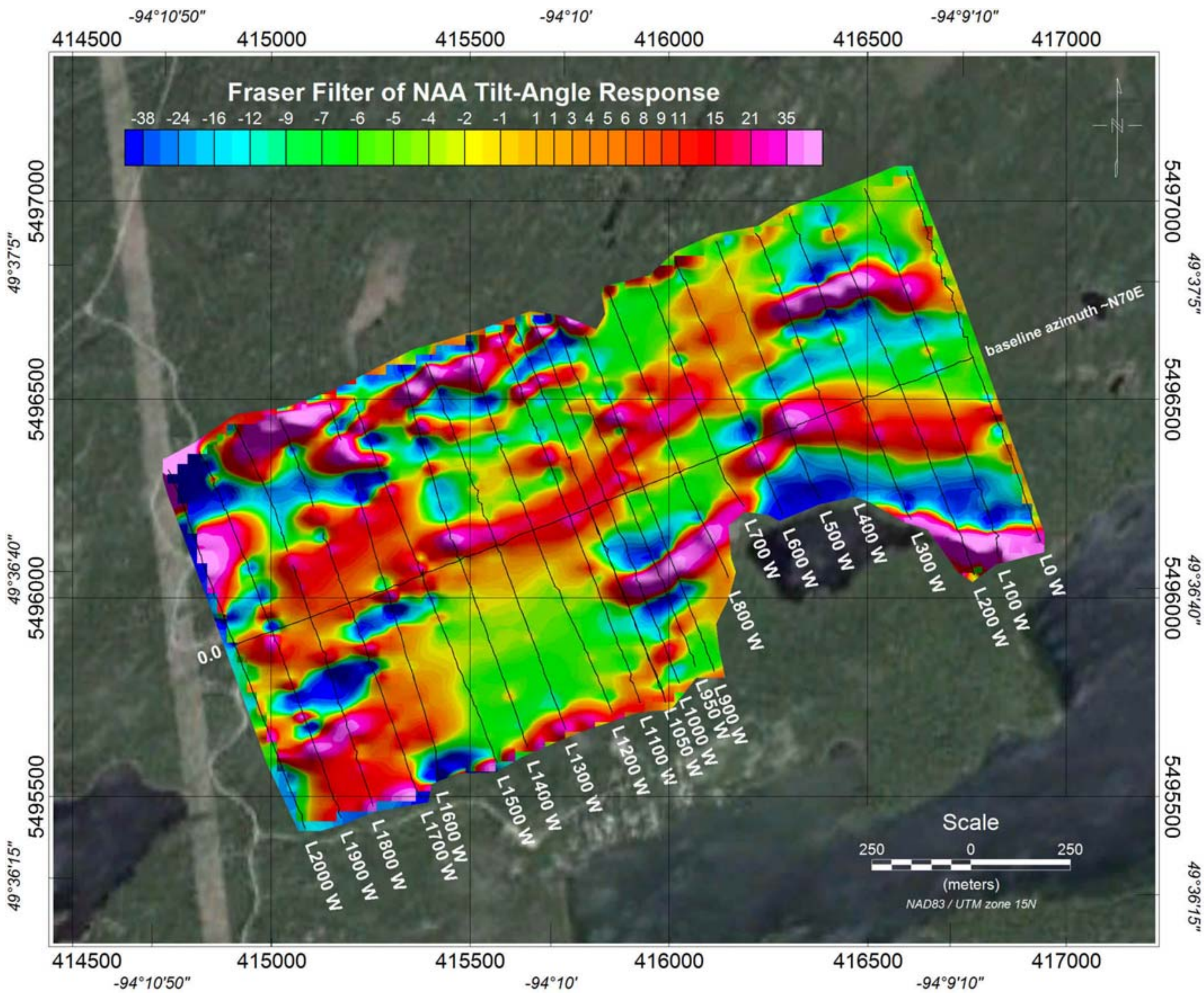

Figure 13. An image of the Fraser Filter plot of the NAA tilt-angle response over the grid area.

Positive regions on the Fraser Filter of the VLF-EM tilt-angle response often overly electrically conductive zones in the subsurface (see Figure 13 above). In many situations, current channelling in the overburden in linear depressions in the bedrock is the main cause of the electrical conductivity. Fracture zones and electrically conductive minerals in the bedrock may also cause these conductors but the majority of these conductors are caused by overburden infilling between bedrock ridges.

It is possible to better understand these conductors by measuring the overburden depth and electrical conductivities with depth within the overburden.

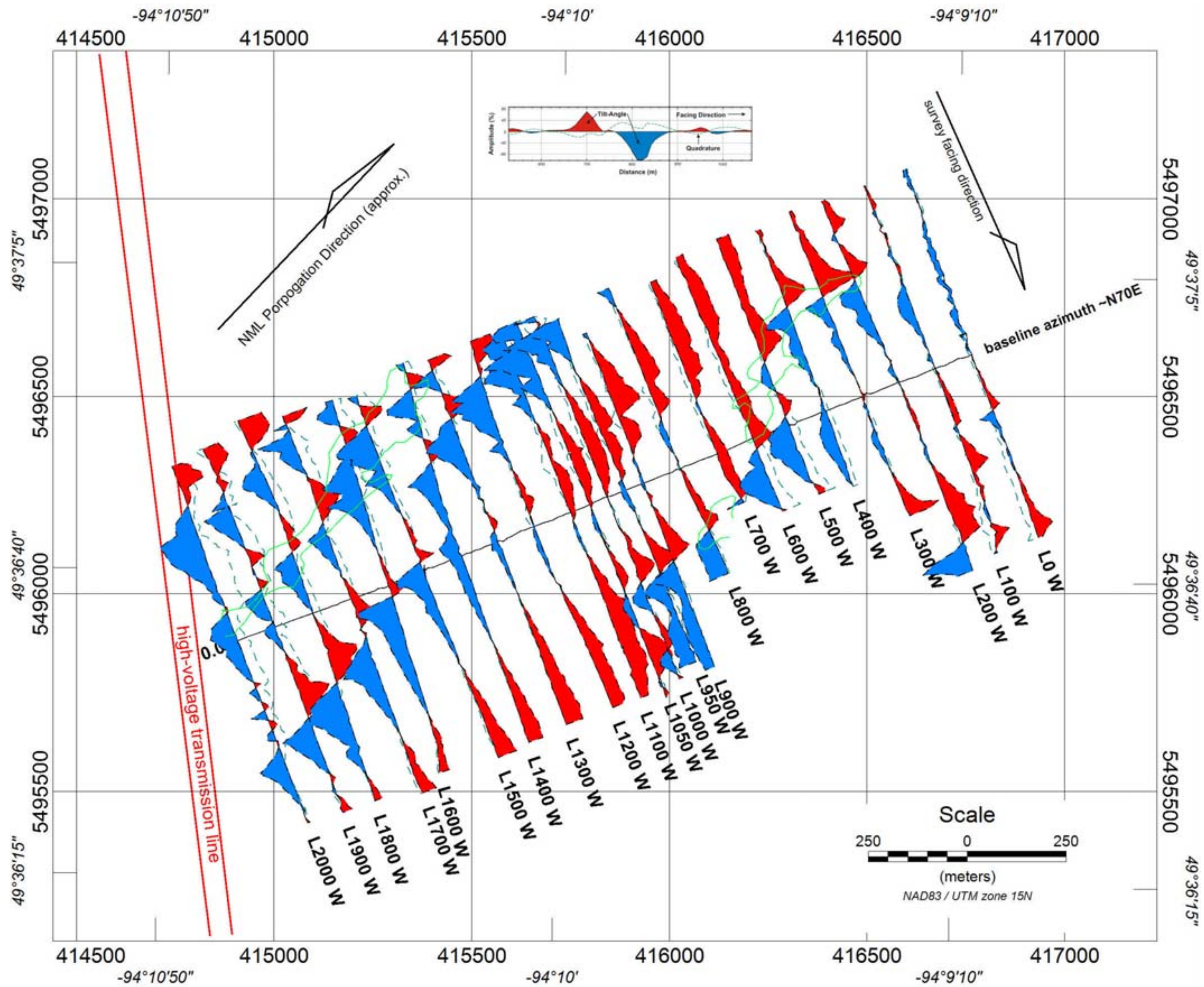

Figure 14. Profiles of the NML tilt-angle and quadrature response are shown here. The survey facing direction is to the south for all lines in this plot.

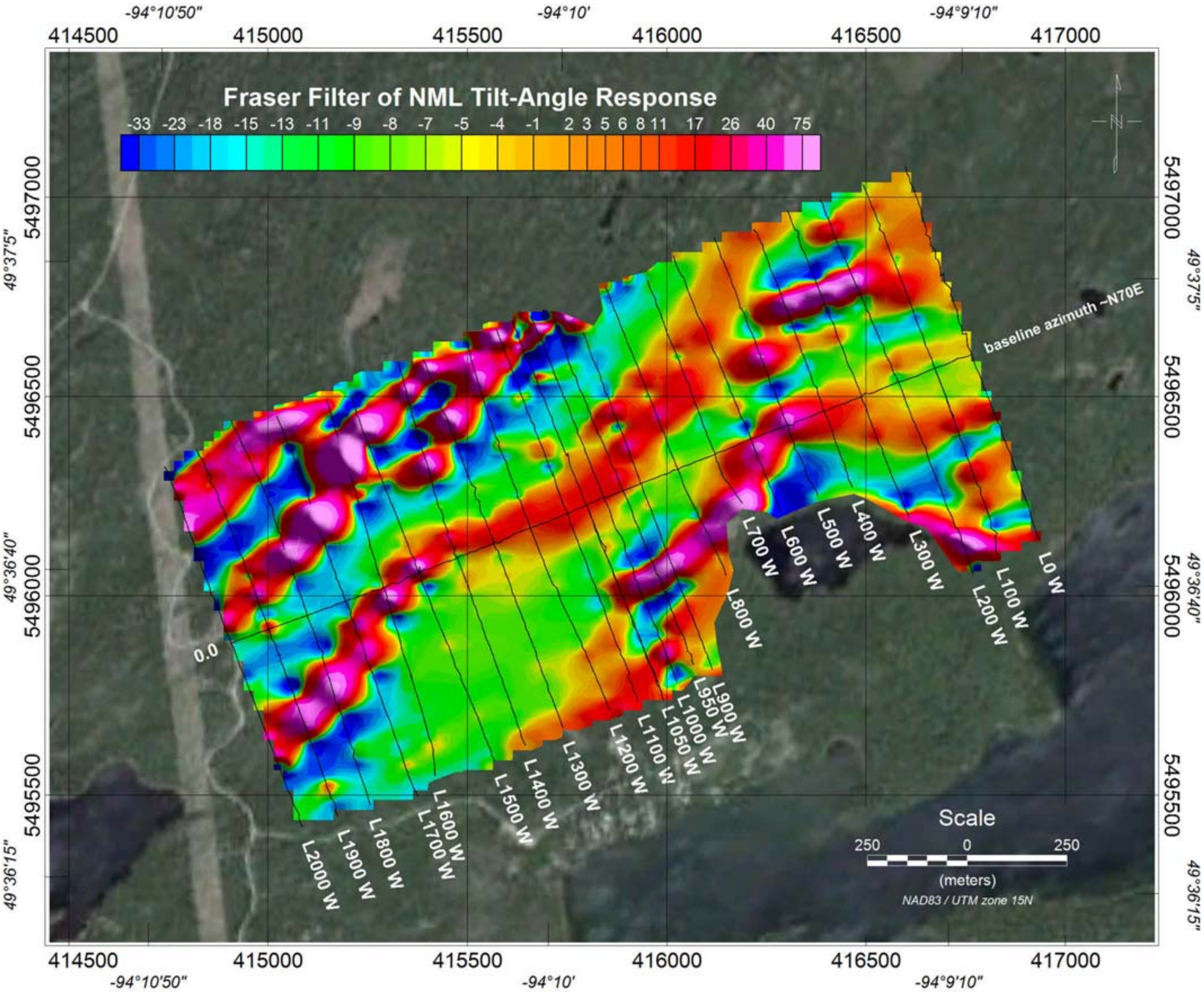

Figure 15. An image of the Fraser Filter plot of the NML tilt-angle response over the grid area.

Areas of positive Fraser Filter values of the VLF-EM tilt-angle response often overly electrically conductive zones in the subsurface (see Figure 15 above). In many situations, current channelling in the overburden in linear depressions in the bedrock is the main cause of the electrical conductivity. Fracture zones and electrically conductive minerals in the bedrock may also cause these conductors but the majority of these conductors are caused by overburden infilling between bedrock ridges.

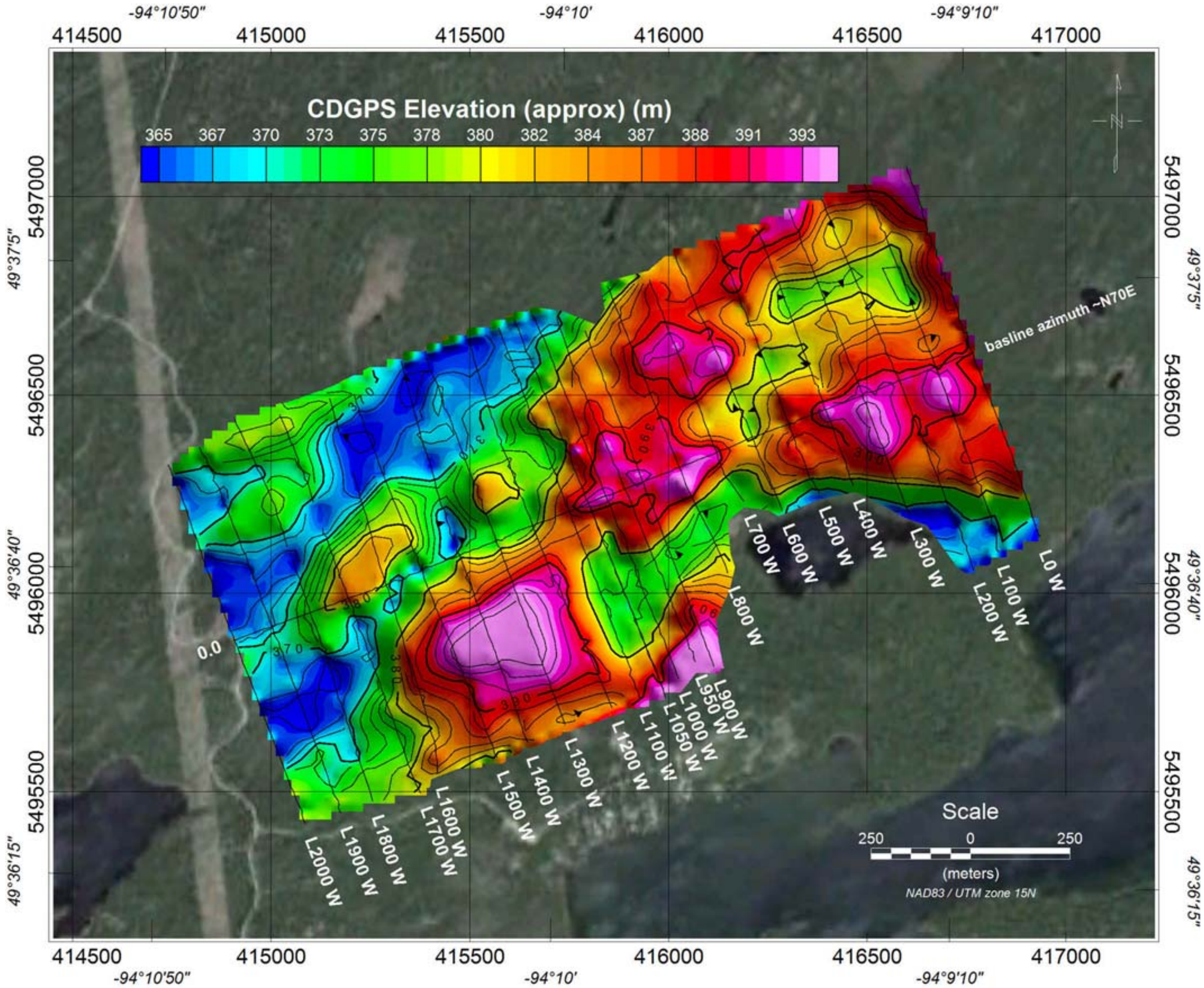

Figure 16. The approximate ground surface topography as measured during the CDGPS survey is shown above.

There is about 40-m of elevation change over the survey grid.

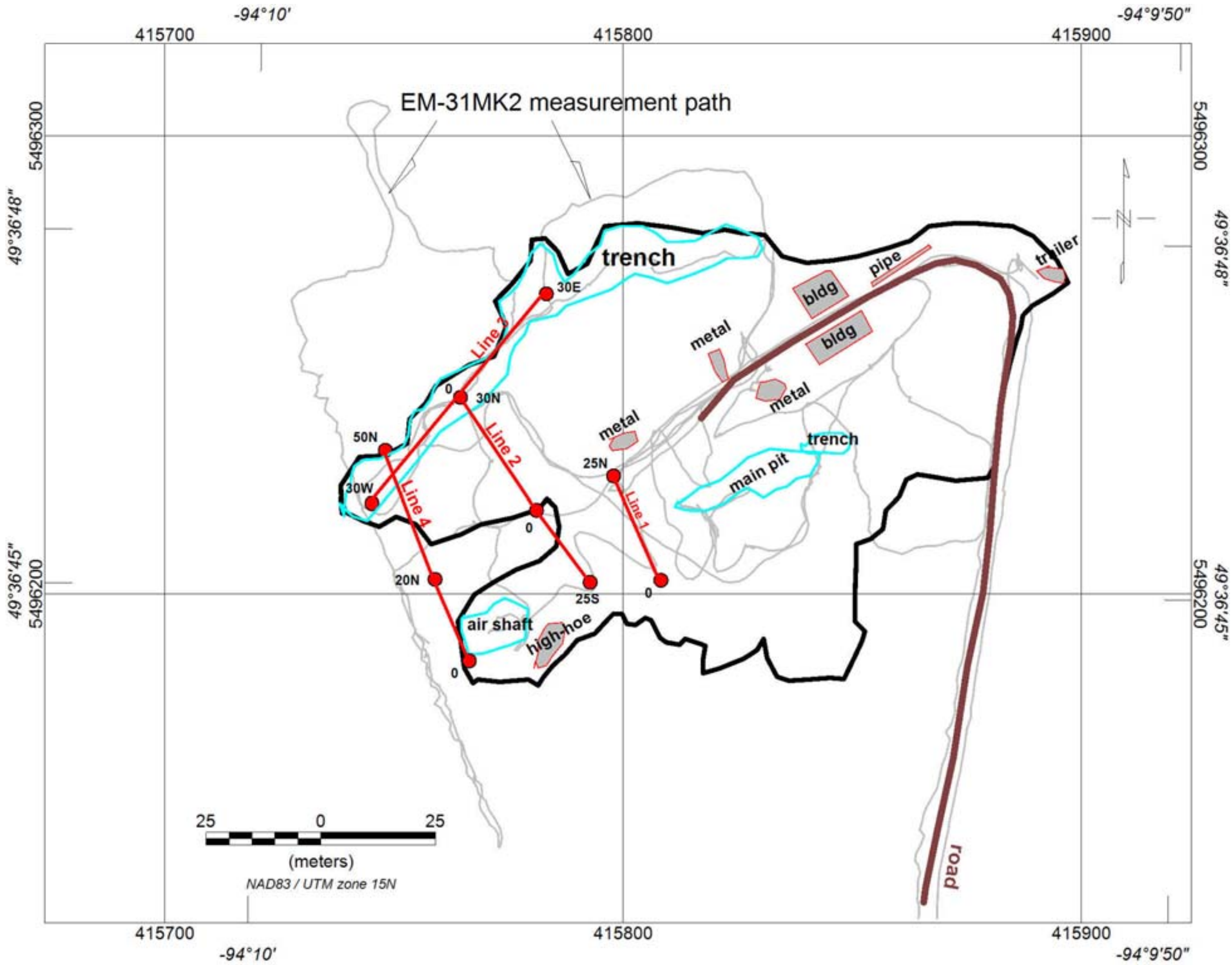

Figure 17. The EM-31MK2 scan was recorded over the main showing area on April 12, 2010. Four detail EM-31 profiles were also collected along Lines 1, 2, 3, and 4 shown above in red on April 13.

The EM-31 scan on April 12 was recorded with the EM-31 antennas in the standard vertical magnetic dipole (VMD) mode which has a signal penetration depth of about 4-m. The apparent electrical conductivity results are plotted in Figure 18 and the in-phase response is shown in Figure 19.

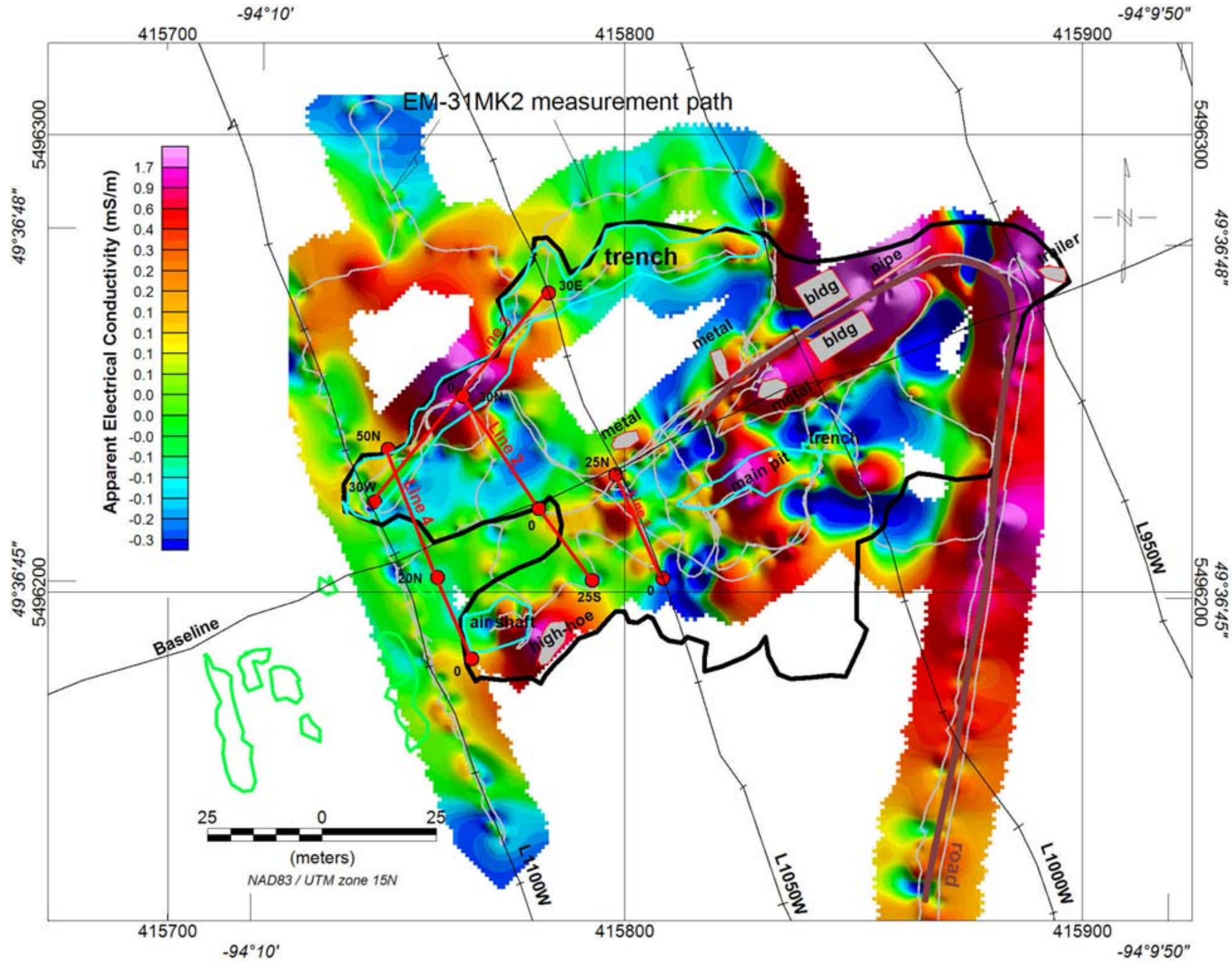

Figure 18. Plot of the EM-31 apparent electrical conductivity from the traverse completed over the main showing area on April 12.

The EM-31 apparent electrical conductivity is very low over this site as would be expected since the bedrock is right at the surface or under shallow sand/gravel overburden. The bedrock is Precambrian age metamorphic volcanic and would be expected to give near-zero EM-31 apparent electrical conductivities (see Table 1). Responses associated with the economic mineral occurrence are not obvious in Figure 18.

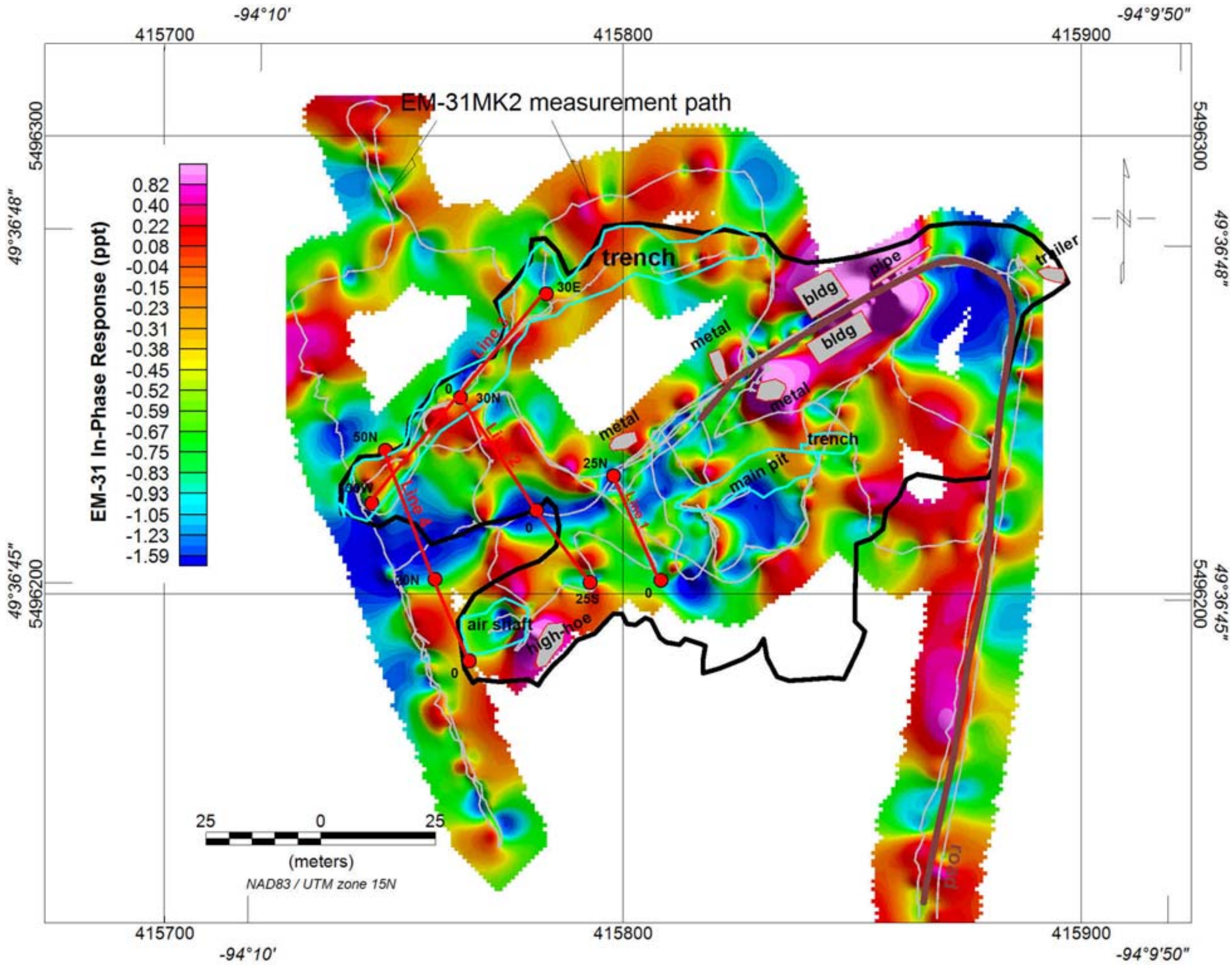

Figure 19. Plot of the EM-31 in-phase response from the April 12 traverse.

The EM-31 in-phase response is also quite low over most of the areas scanned in the showing area (see Figure 18). Most of the highs in the in-phase are caused by metal objects nearby.

For the detail EM-31 profiles along Lines 1, 2, 3, and 4 on April 13 the EM-31 response was recorded for both the vertical magnetic dipole (VMD) and horizontal magnetic dipole (HMD) modes at two orientations in-line and cross-line (see Figures 10 to 13 below). Responses associated with the economic mineral occurrence are not obvious in Figure 19.

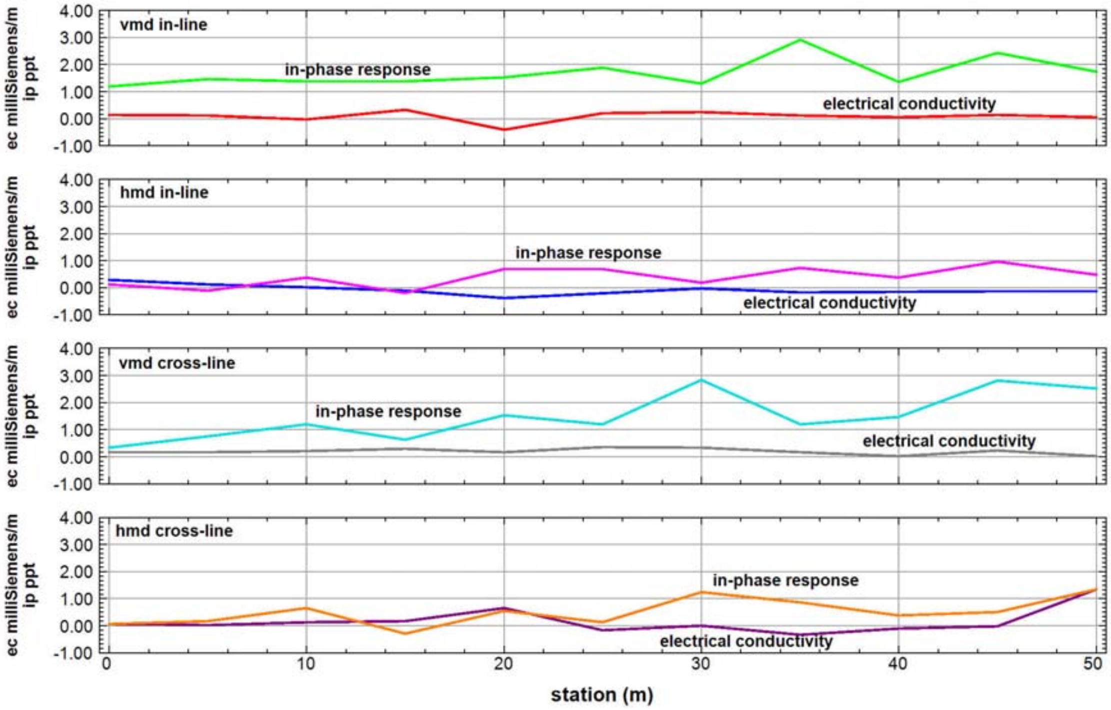

Figure 20. Plot of the detail EM-31 profiles for Line 1 on April 13.

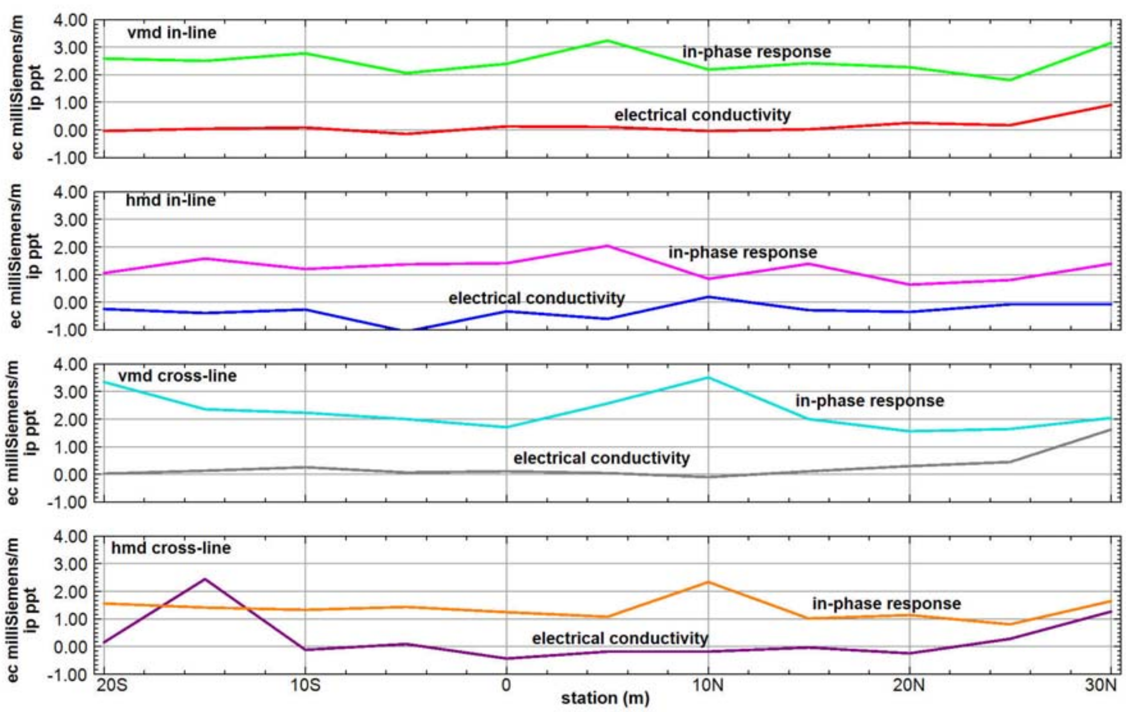

Figure 21. Plot of the detail EM-31 profiles for Line 2 on April 13.

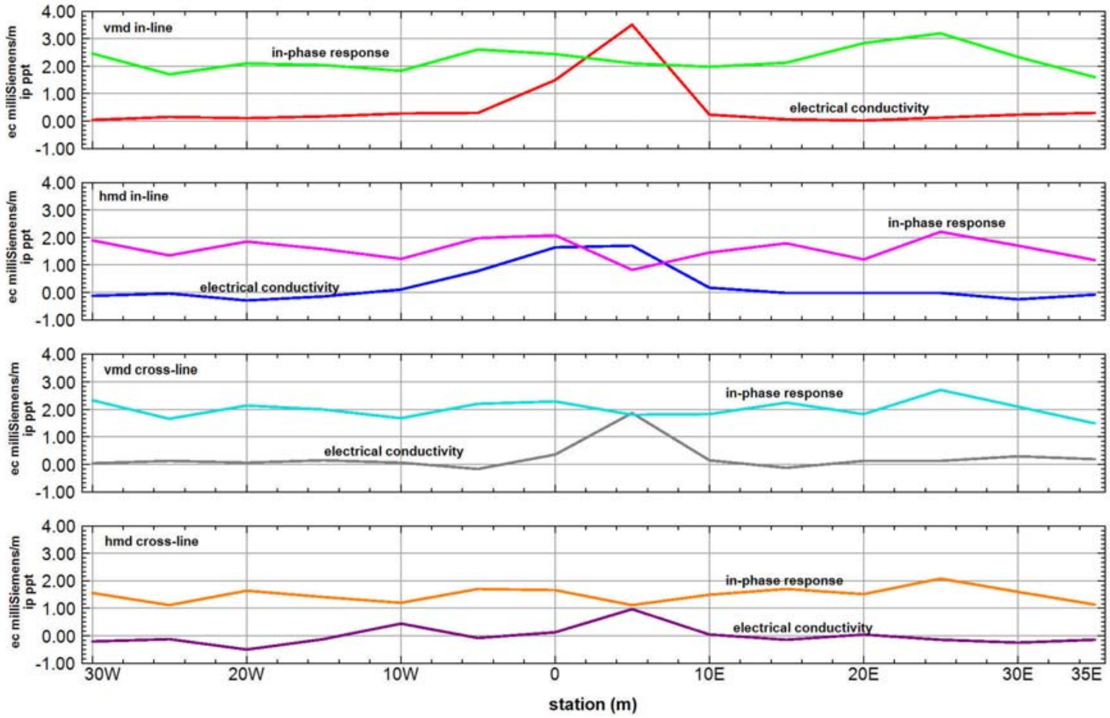

Figure 22. Plot of the detail EM-31 profiles for Line 3 on April 13.

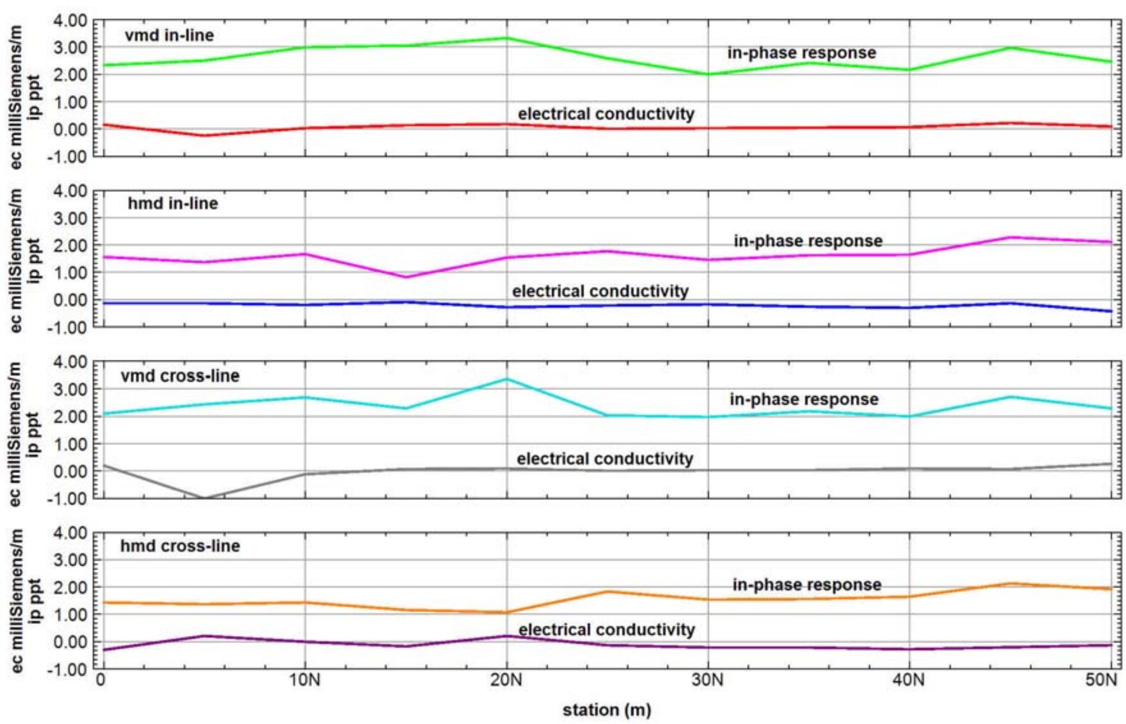

Figure 23. Plot of the detail EM-31 profiles for Line 4 on April 13.

The apparent electrical conductivities observed in Figures 20 to 23 are all about 0 milliSiemens/metre as would be expected over PreCambrian metamorphic volcanic bedrock that may have disseminated metallic minerals but these metallic minerals are isolated from each other do not form an electrical continuity over distances of 0.5-m to 5-m. Station 5E on Profile 3, which runs along a trench, is the only area where the apparent electrical conductivity increases and may indicate disseminated metals or a water-filled shear. A metal object hidden from view like drill steel may also cause this response.

Interpretation and Discussion

Interpretations of geophysical survey results are rarely unique; ground-truth in the form of surficial mapping, drilling or excavation is needed to increase confidence in the model suggested from the geophysics. The non-uniqueness in geophysical interpretation is particularly true at the early stages of exploration when little is known of the physical properties in the subsurface.

One of the assumptions in the interpretation of magnetic responses at the early reconnaissance stage is that remnant magnetization is negligible for the magnetic minerals.

Figure 24 shows a histogram and lists the standard statistics for the 1919 total magnetic field measurements on the grid.

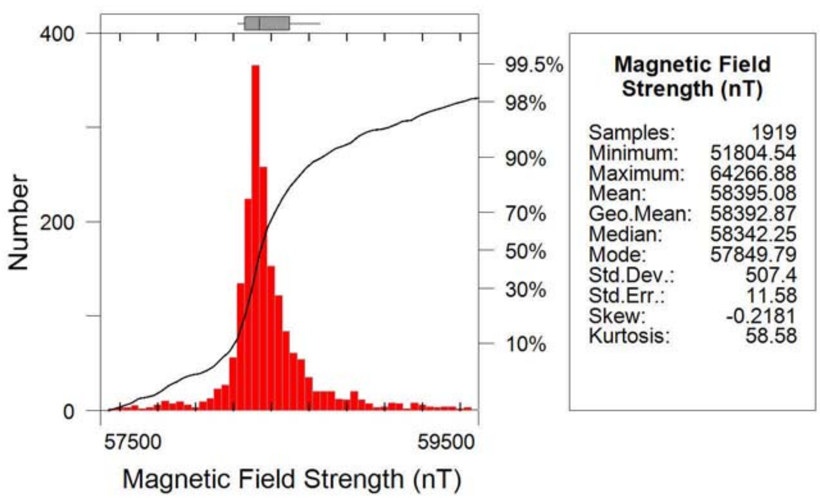

Figure 24. A histogram of the total magnetic field strength for all the 1900 measurements is shown above.

The mean magnetic field is 58,395 ± 507 nT for the 1919 measurements recorded on this grid. The magnetic field strength ranges over 13,400-nT from a low of 51,800-nT to a high of over 64,200-nT. This large range along with the large standard deviation of over 500-nT means there are significant concentrations of magnetite and significant variation in magnetite. Magnetite concentrations probably vary from 1% to 50% (by volume) in the bedrock.

Another observation about the magnetic field on this grid is its irregularity. Estimating the local rock fabric, local strike and dip, is not easy from the magnetic field. Figure 9 shows little line to line correlation in the magnetic field even in the central area where the line separation is 50-m. Another characteristic is there seems to be more strong magnetic lows without attendant highs on this property. There are highs associated with lows but they are complex and do not lend themselves to the typical dipping dyke-like models used so often in magnetic interpretation. Profile plots of the magnetic field show that the 12.5-m measurement spacing along the survey lines may be too large in some places.

All of these observations on the magnetic field (see Figure 9) suggest irregular bands of up to 50% magnetite occur over the property and could be easily observed in hand or core sample. The strong lows also suggest remnant magnetization may be a factor on this property.

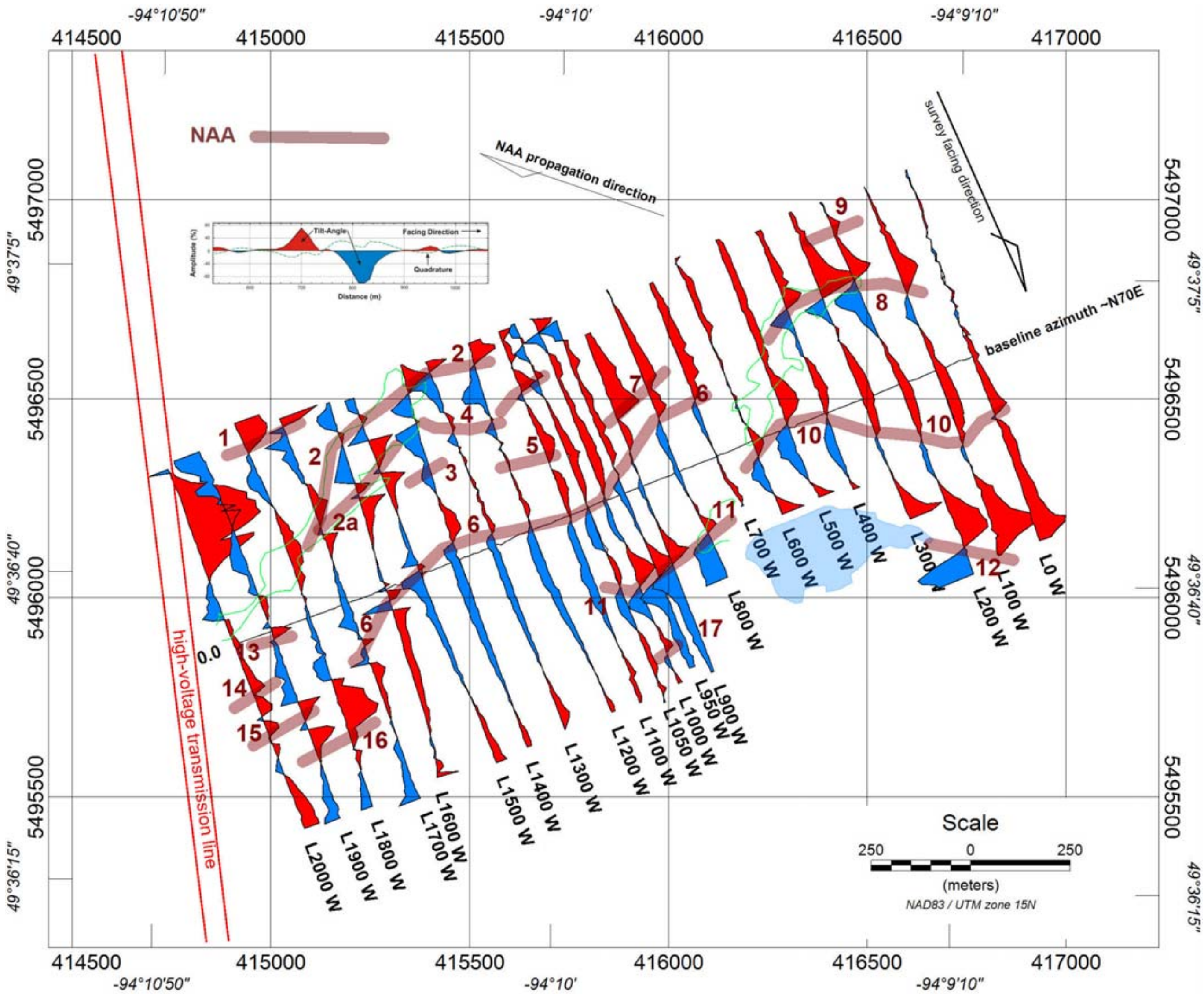

Figure 25. Seventeen VLF conductor axes are interpreted in the NAA survey.

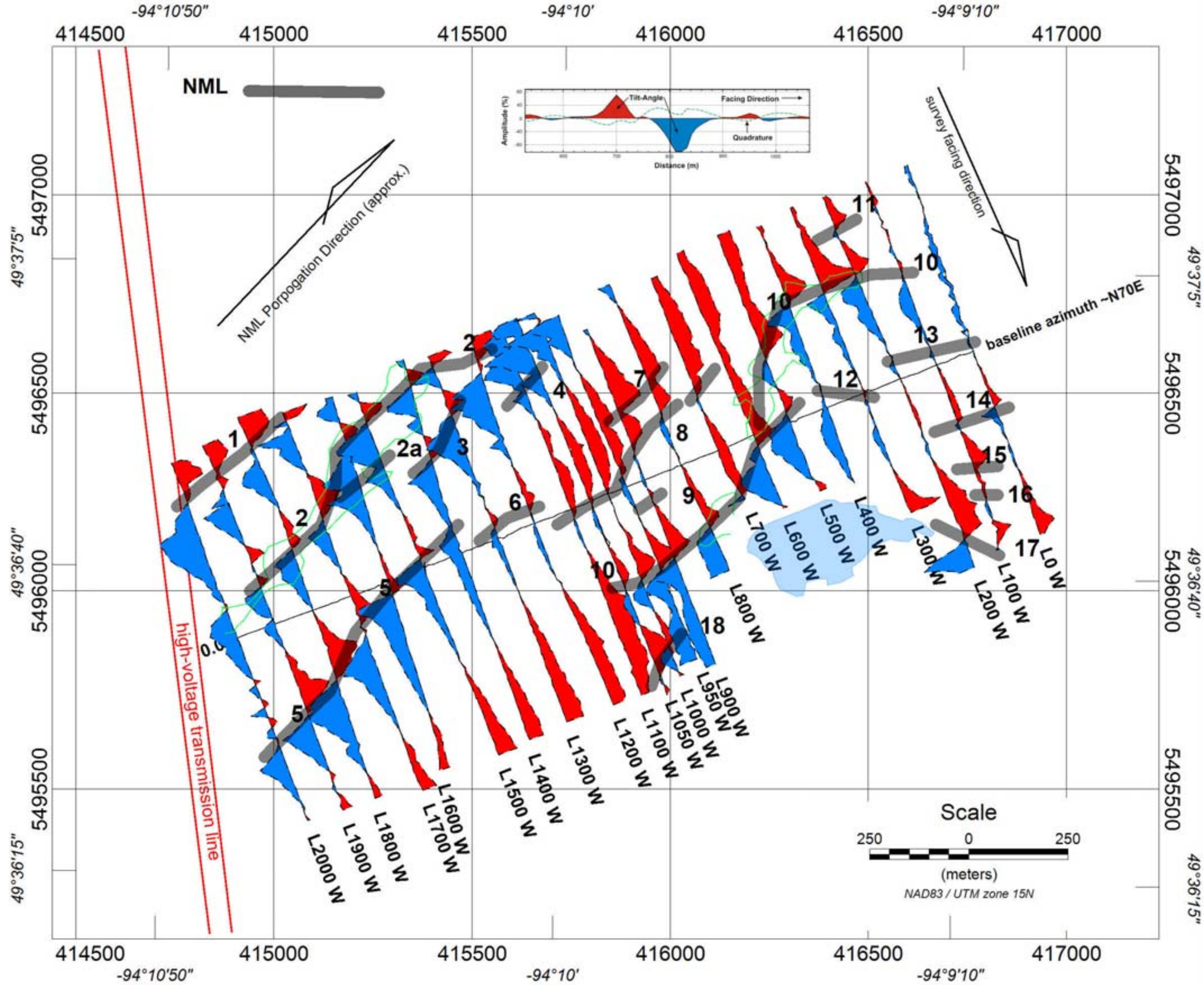

Figure 26. Eighteen conductors are interpreted on the NML survey data.

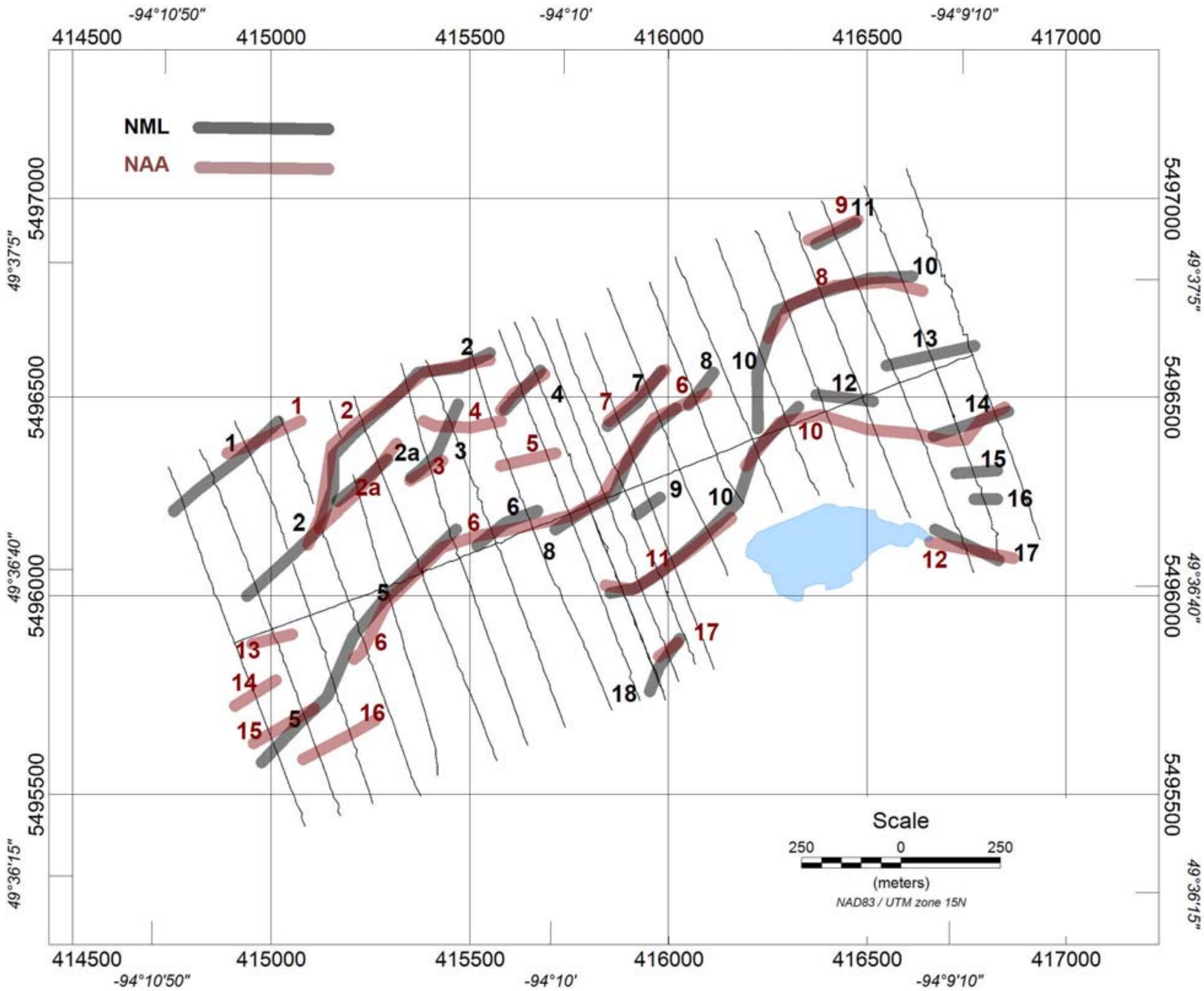

Figure 27. Seventeen NAA and 18 NML conductor axes have been classified on the property.

Figure 27 shows that many NAA conductors are also NML conductors. There is quite a difference in signal propagation direction between NAA and NML so these conductors probably have a bedrock influence.

VLF conductors are common in the Canadian Shield and the figure below presents a common predicament in VLF interpretation. Electrical current channelling in overburden-filled valleys between bedrock ridges are the most common VLF-conductor in the Canadian Shield. Figure 14 below presents a schematic of effect with approximate electrical resistivities shown.

The electrical resistivity of Precambrian bedrock is often 50 to 100 times greater than the overburden. This means that VLF currents will tend to flow preferentially in the less-resistive or more-conductive overburden. Fractures in the bedrock, will often reduce the electrical conductivity locally by a factor of 10. When a VLF conductor is observed on an exploration project it is important to understand how much of the current is due to the overburden and how much is caused by current flow in the subsurface fracture or mineralized structure.   The answer to this question requires knowledge of the overburden thickness and electrical properties and the ability to model the VLF-EM field response. Subsurface electrical properties are very important to anyone attempting to 'explain' VLF conductors. Downhole physical property measurements would be a big help in this case.

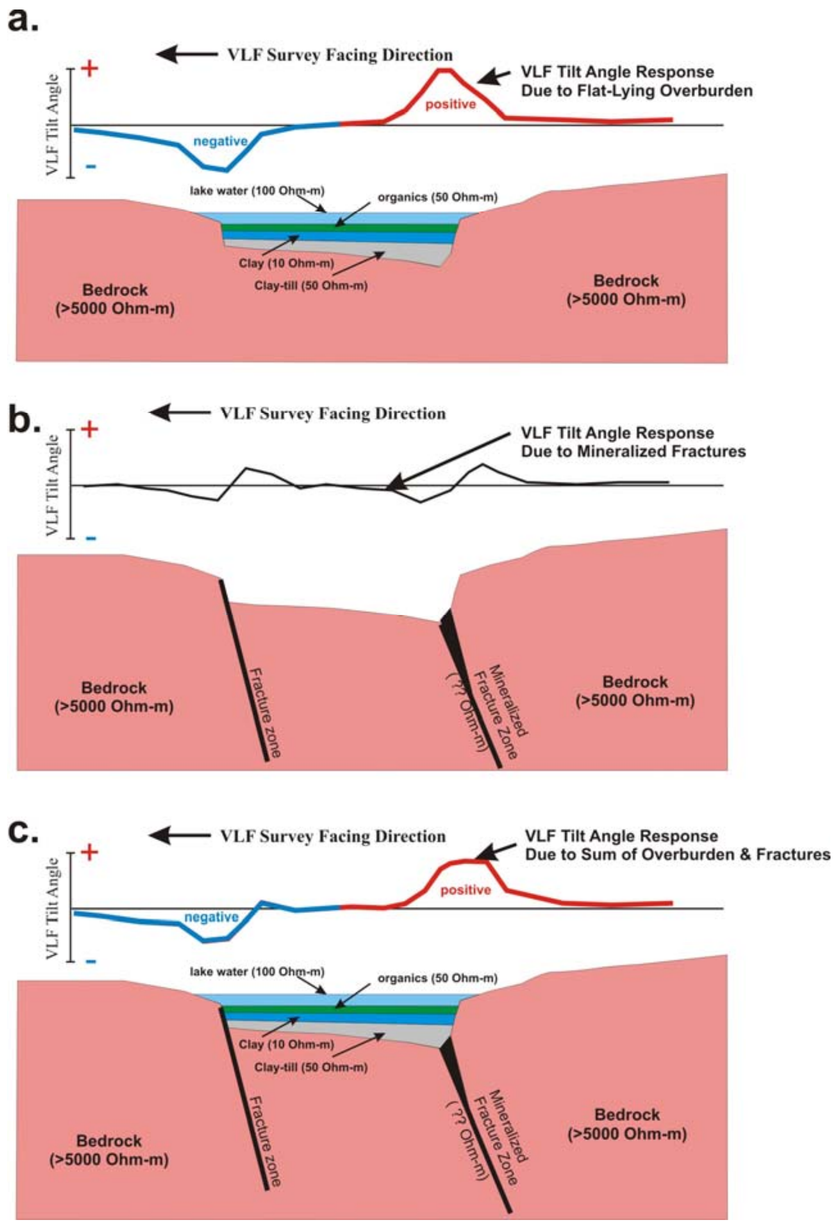

Figure 28. (a) Electrically conductive surficial deposits in valleys tend to channel VLF currents preferentially between the highly electrically resistive bedrock ridges. Fracture zones (b) may often be the cause of these abrupt bedrock interfaces but it is difficult to know how much of the observed VLF response (c) is due to current flow in the fracture and how much is caused by current flow in the overlying overburden.

Figure 28 illustrates a difficulty in interpreting bedrock structures in VLF data. In Figure 28a an approximate response of the lake and lake-bottom sediments is shown. Figure 28b shows weak responses associated with mineralized and electrically conductive fracture zones and 28c shows the sum of the two effects. More physical property measurements and depth-to-bedrock measurements would help to better understand VLF responses.

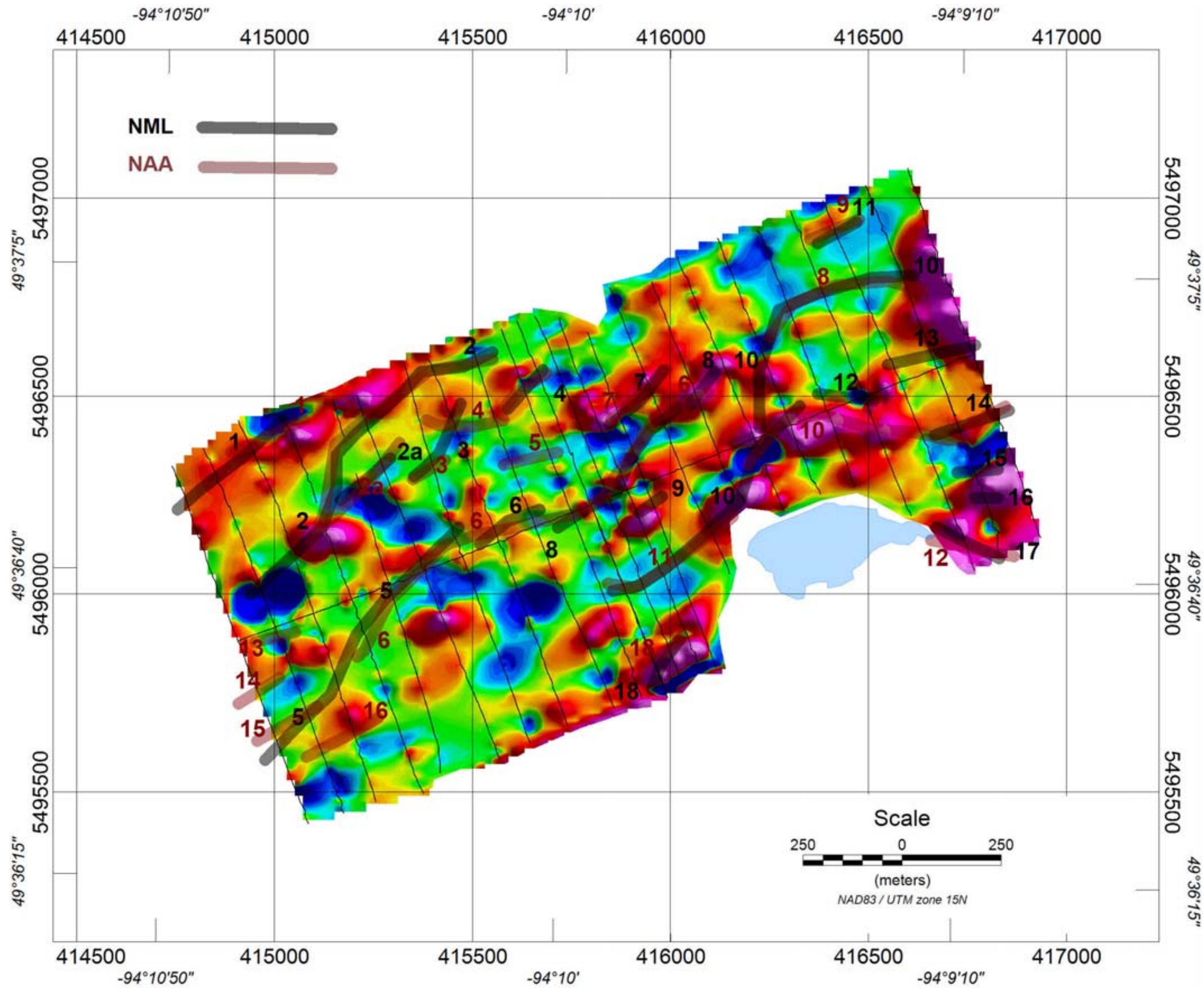

Figure 29. VLF conductors are superimposed on the total magnetic field.

The magnetic field does not compare very well with the VLF conductors.

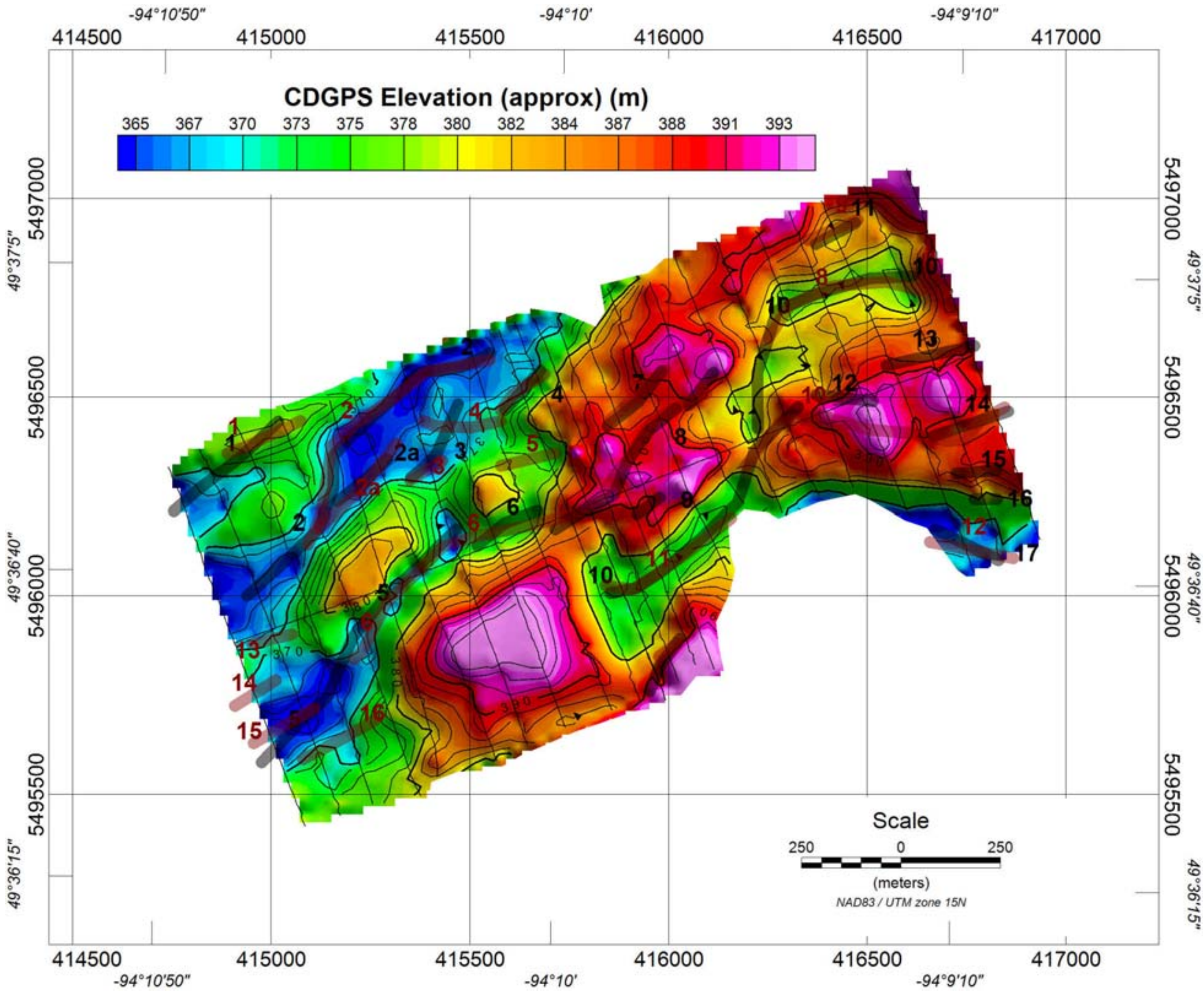

Figure 30. VLF conductors superimposed on the topography.

Figure 30 is interesting as it shows good correlation between VLF conductors and valleys. This is no surprise as electrically conductive overburden probably in-fills these valleys but bedrock conductors like fracture zones as illustrated in Figure 28 may also contribute. Conductors that do not fit the conductor-in-a-valley model, like 7, 8, and 9 in Figure 30 may be worth more attention. Conductor 8 is interesting because it coincides approximately with the central showing.

Conclusions and Recommendations

About 1900 measurements of the total magnetic field and the VLF-EM field from two separate transmitters have been recorded along 23.7-km of line from April 7 to 13, 2010. These measurements were recorded at approximately 12.5-m intervals with a horizontal accuracy of about ±0.5-m. The DGPS measurements also permitted the recording of the approximate topography profile along each line and this data has also been presented.

An EM-31MK2 survey was also completed over the open areas over the showing area and four detail EM-31MK2 profiles were recorded. The EM-31 is essentially a horizontal-loop EM system with a 3.6-m coil separation operating at 9800-Hz and can assist in locating massive sulphide concentrations within 2 to 3-m of surface in the showing area. Some mapping of claim posts, claim lines and trenches has also been completed.

The magnetic survey map shows a strong and erratic magnetic field that does not correlate well line to line. Bands of magnetite must be fairly common and are irregularly distributed in the bedrock. Patterns in the magnetic field do not correlate well with the topography or the VLF-EM fields. There are some very strong magnetic lows without an attendant high and this may indicate a remnant magnetization that is perhaps in the opposite direction to the present Earth's field. The strong and erratic nature of the magnetic field is a significant geological characteristic of the rocks here. The variations in magnetite should be easily observed in comparisons between hand-size samples.

The EM-31MK2 scan and profiles show the apparent electrical conductivity is, as expected, very low over the showing area. The in-phase response is also quite subdued. There does not appear to be any anomalous EM-31 responses that could be attributed to metallic metal sulphides.

About 18 VLF EM conductors have been interpreted over the gird and many of these conductors were observed on both the NAA and NML surveys. Many of these conductors are probably caused by electrically conductive overburden infilling bedrock ridges but there are conductors in the showing area that appear to cut across topographic highs and these may warrant further study.

If exploration drilling is completed it would be useful if downhole physical property measurements were completed or if measurements were recorded along the core. Downhole probes measure larger volumes and better representative measurements than that made on core samples. But, in the absence of downhole measurements, physical property measurements on core are the next best thing. Measurements of magnetic susceptibility, natural gamma, and induced-polarization-electrical resistivity would be quite useful. Having a good estimate of the magnetic susceptibility downhole would provide a better modelling capability and greater confidence in predicting the size and geometry of the magnetic zones here.

Exploration in the future will have to pay more attention to physical property measurements to serve as standard input to the 2D and 3D physical models that are available. This may help improve the 'anomaly chasing' mode that more often guides exploration.

Modelling of VLF-EM responses is recommended if the overburden thickness and the electrical conductivity of the overburden is better defined.

Acknowledgements

John Burt helped with access to the property.

respectfully submitted,

John Hayles P.Eng. P.Geo.
Geophysicist
Hayles Geoscience Survey Ltd.
511 Robinson Avenue
Selkirk, Manitoba
R1A 1E5
phone (204) 482 5249
www.haylesgeoscience.ca

Date: July 14, 2010

References:

Beck, A.E. 1991. Physical Principles of Exploration Methods. Wuerz Publishers 292p.

Geonics Ltd. EM-61 High-Sensitivity Metal Detector – Operating Manual

Grant, F.S. and G.F. West. 1965. Interpretation Theory in Applied Geophysics. McGraw Hill 584p.

Hayles, J. G. 2010. Operator's Report: Ground Magnetometer, VLF-EM and EM-31MK2 Surveys – Olympian Gold Project – Triggs Mine Area Grid – April 7 to 13, 2010. Hayles Geoscience Surveys Ltd Report to Nuinsco Resources Ltd. 17 p.

McNeill, J.D. 1980. Electrical Conductivity of Soils and Rocks. Technical Note TN-5, Geonics Ltd

McNeill, J.D. 1980. Electromagnetic terrain conductivity measurement at low induction numbers. Technical Note TN-6, Geonics Ltd

McNeill, J.D. 1980. EM34-3 Survey Interpretation Techniques. Technical Note TN-8, Geonics Ltd.

McNeill, J.D. and V.F. Labson. 1991. Geological Mapping using VLF Radio Fields. in Electromagnetic Methods in Applied Geophysics. Volume 2, Applications part B. page 521-640 Society of Exploration Geophysicists.

Telford, W.M., L.P Geldart, and R.E. Sheriff, 1993. Applied Geophysics (2nd edition) Cambridge University Press 770p.

Appendix

Table A-1 below lists the daily survey production over the grid.

Table A-1: Production – Grid Survey

date	line	start (m)	end (m)	distance (m)	per-day (m)	points
April 7, 2010	1050W	-500	0	500		
	Baseline	1050	0	1050		
	0W	500	-500	1000		
	100W	-500	0	500	3050	244
April 8, 2010	100W	-125	500	625		
	200W	500	-500	1000		
	300W	-337.5	500	837.5		
	400W	500	-200	700		
	500W	-200	500	700		
	600W	500	62.5	437.5	4300	344
April 9, 2010	600W	50	-200	250		
	700W	-150	462.5	612.5		
	800W	500	-300	800		
	900W	-500	475	975		
	950W	525	-475	1000		
	1000W	-500	500	1000		
	1050W	500	0	500	5137.5	411
April 10, 2010	1050W	0	-525	525		
	1100W	-500	487.5	987.5		
	1200W	500	-500	1000		
	1300W	-500	500	1000		
	1400W	-500	500	1000		
	1500W	-500	0	500	5012.5	401
April 11, 2010	baseline	2000	1050	950		
	1500W	0	387.5	387.5		
	1600W	300	-500	800		
	1700W	-500	187.5	687.5		
	1800W	137.5	-500	637.5		
	1900W	-500	500	1000		
	2000W	500	0	500	4962.5	397
April 13, 2010	2000W	0	-500	500		
	1800W	500	150	350		
	1700W	262.5	500	237.5		
	1600W	500	400	100		
	1500W	425	500	75	1262.5	101
			Total	**23725**	**23725**	**1898**

Figure A-1 shows the magnetic field strength recorded by the base station of each of the survey days. The base station was located at coordinates: ***(416033.0E, 5495658.9N)*** using the NAD83 datum and UTM Zone 15N.

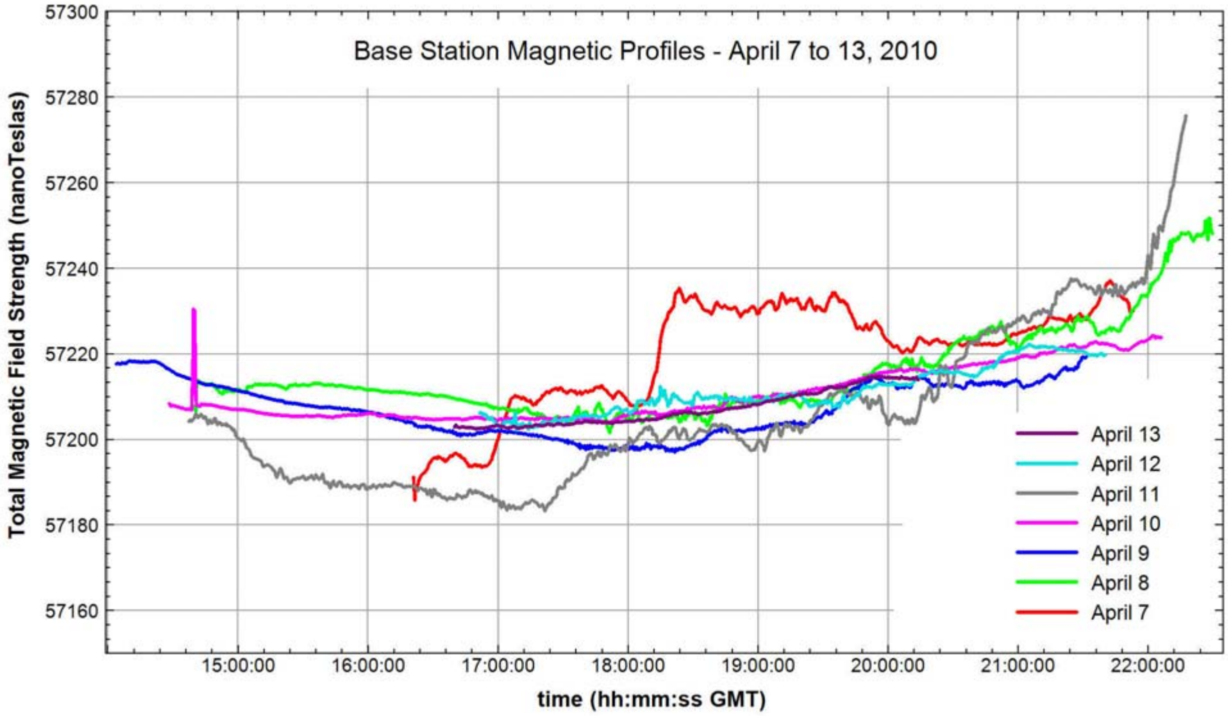

Figure A-1. A plot of the magnetic field strength measured every 30-s at the base station for each day of survey is shown above.

Sun spot activity, which generates the solar wind of charged ions streaming past the earth, influences the magnetic fields on earth, and has been unusually quiet recently. Moving ionic charges constitute an electrical current and all electrical currents have an associated magnetic field. The earth's magnetic field is then constantly buffeted by a variable magnetic field generated by the sun. The variations in the magnetic field observed on April 7 have been confirmed with comparisons to the magnetic base station in Brandon, Manitoba by the Geological Survey of Canada.

Statement of Qualifications

I, John G. Hayles, completed the survey. I graduated from Queen's University in 1970 with the degree of Bachelor of Science in Geological Engineering (geophysics option). I have a Master of Applied Science in Geophysics from the University of B.C. in 1973 and have been working continually in exploration geophysics in Canada since then. I am a professional engineer registered with Professional Engineers Ontario since 1975 (member 18936013) and am registered as a professional geoscientist and engineer with the Association of Professional Engineers and Geoscientists Manitoba (member 20222). I am member of the Society of Exploration Geophysicists, the Geological Association of Canada, the Canadian Geophysics Union, the American Geophysics Union and the European Association of Exploration Geophysicists.

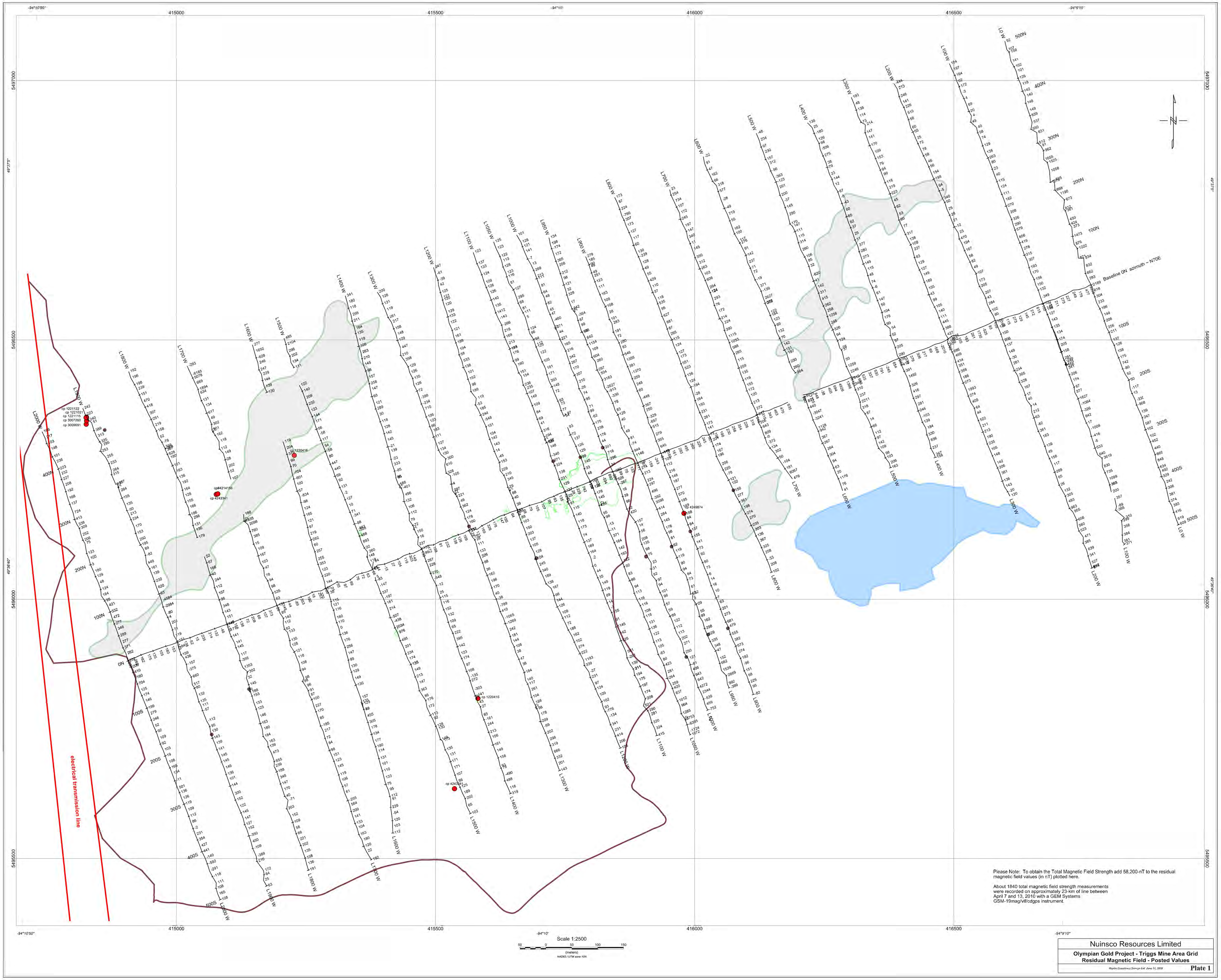
415000
415500
416000
416500
5497000
5496500
5496000
5495500
-94°10'50"
-94°10'
-94°9'10"
Baseline 0N azimuth = N70E
electrical transmission line
Scale 1:2500
(meters)
NAD83 / UTM zone 15N
Please Note: To obtain the Total Magnetic Field Strength add 58,200-nT to the residual magnetic field values (in nT) plotted here.
About 1840 total magnetic field strength measurements were recorded on approximately 23-km of line between April 7 and 13, 2010 with a GEM Systems GSM-19mag/vlf/cdgps instrument.
Nuinsco Resources Limited
Olympian Gold Project - Triggs Mine Area Grid
Residual Magnetic Field - Posted Values
Hayles Geoscience Surveys Ltd June 21, 2010
Plate 1

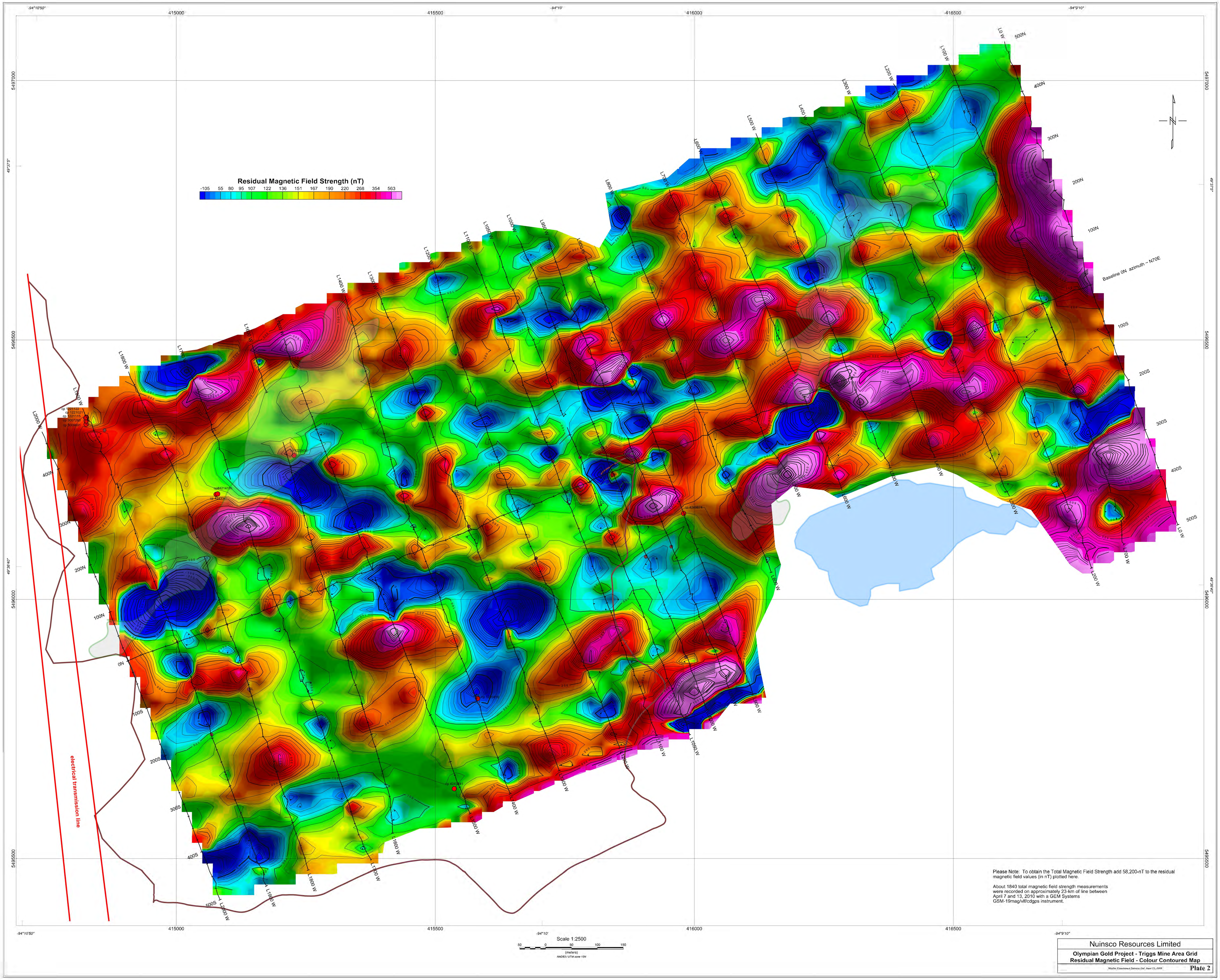
Residual Magnetic Field Strength (nT)
-105 55 80 95 107 122 136 151 167 190 220 268 354 563
Baseline 0N azimuth ~ N70E
electrical transmission line
Scale 1:2500
(meters)
Please Note: To obtain the Total Magnetic Field Strength add 58,200-nT to the residual magnetic field values (in nT) plotted here.
About 1840 total magnetic field strength measurements were recorded on approximately 23-km of line between April 7 and 13, 2010 with a GEM Systems GSM-19mag/vlf/cdgps instrument.
Nuinsco Resources Limited
Olympian Gold Project - Triggs Mine Area Grid
Residual Magnetic Field - Colour Contoured Map
Plate 2

Nuinsco Resources Limited

Olympian Gold Project - Triggs Mine Area Grid
VLF-EM Posted Measurements from Station NAA

Hayles Geoscience Surveys Ltd June 28, 2010 **Plate 3**

Nuinsco Resources Limited

Olympian Gold Project - Triggs Mine Area Grid
VLF-EM Posted Measurements from Station NML

Plate 4

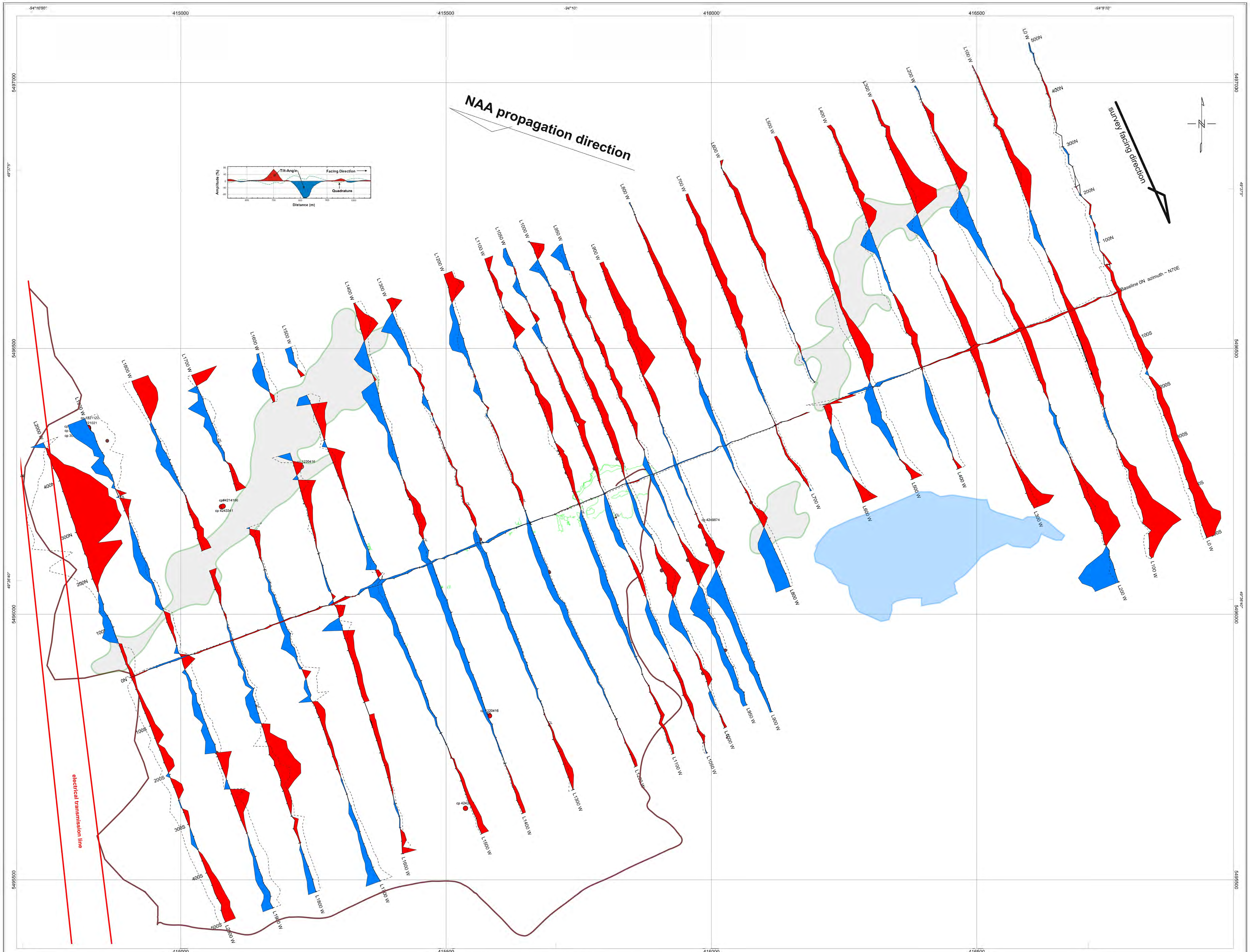

Nuinsco Resources Limited

Olympian Gold Project - Triggs Mine Area Grid
VLF-EM Tilt-Angle and Quadrature Profiles

Hayles Geoscience Surveys Ltd June 28, 2010

Plate 5

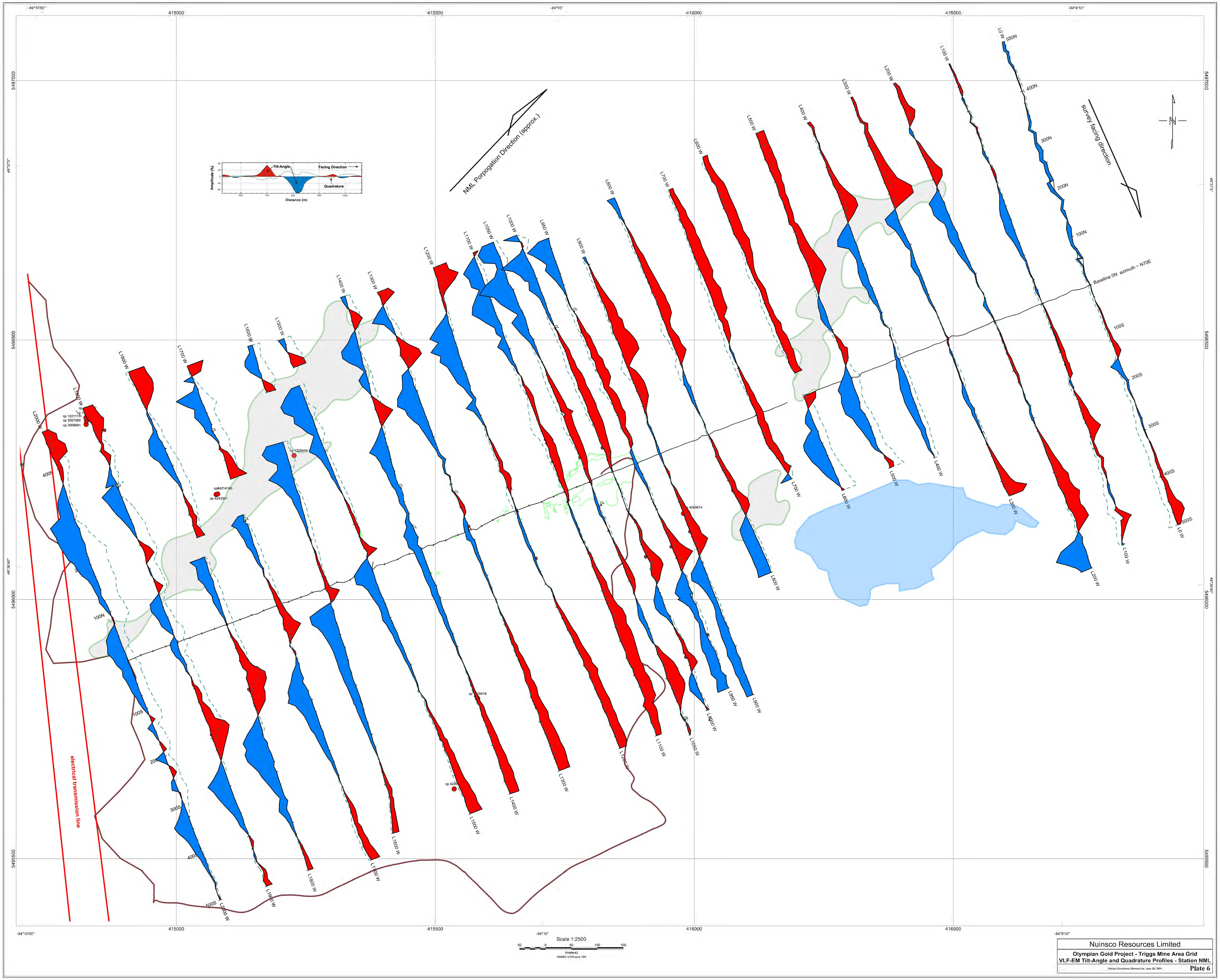

NML Porpogation Direction (approx.)
survey facing direction
Tilt-Angle
Facing Direction
Quadrature
Amplitude (%)
Distance (m)
Baseline 0N azimuth = N70E
electrical transmission line
415000
415500
416000
416500
5497000
5496500
5496000
5495500
-94°10'50"
-94°10'
-94°9'10"
Scale 1:2500
(meters)
Nuinsco Resources Limited
Olympian Gold Project - Triggs Mine Area Grid
VLF-EM Tilt-Angle and Quadrature Profiles - Station NML
Plate 6

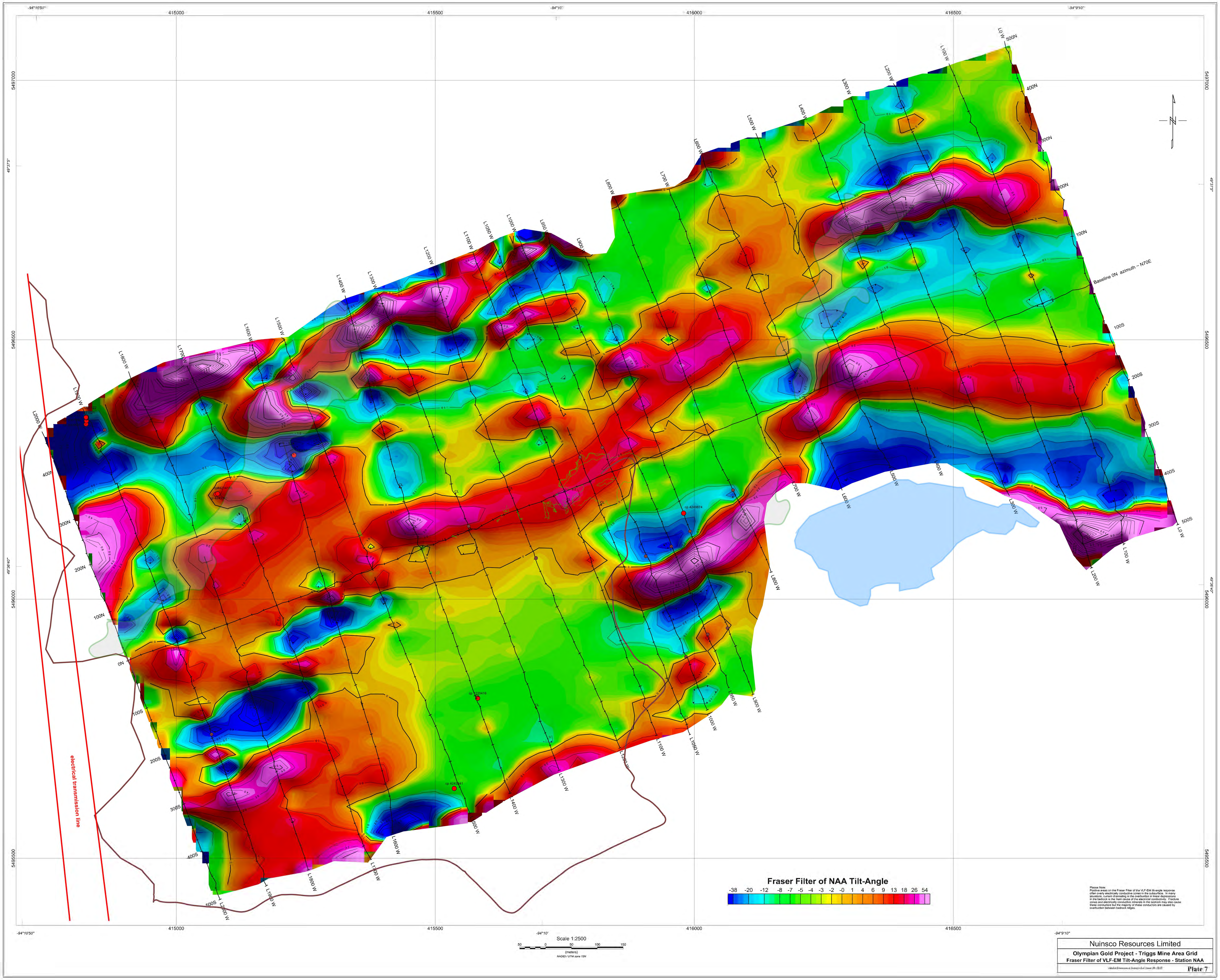

Fraser Filter of NAA Tilt-Angle
-38 -20 -12 -8 -7 -5 -4 -3 -2 -0 1 4 6 9 13 18 26 54
electrical transmission line
Baseline 0N azimuth ~ N70E
Scale 1:2500
(meters)
415000
415500
416000
416500
5497000
5496500
5496000
5495500
-94°9'10"
Please Note:
Positive areas on the Fraser Filter of the VLF-EM tilt-angle response often overly electrically conductive zones in the subsurface. In many situations, current channeling in the overburden in linear depressions in the bedrock is the main cause of the electricial conductivity. Fracture zones and electrically conductive minerals in the bedrock may also cause these conductors but the majority of these conductors are caused by overburden between bedrock ridges.
Nuinsco Resources Limited
Olympian Gold Project - Triggs Mine Area Grid
Fraser Filter of VLF-EM Tilt-Angle Response - Station NAA
Plate 7

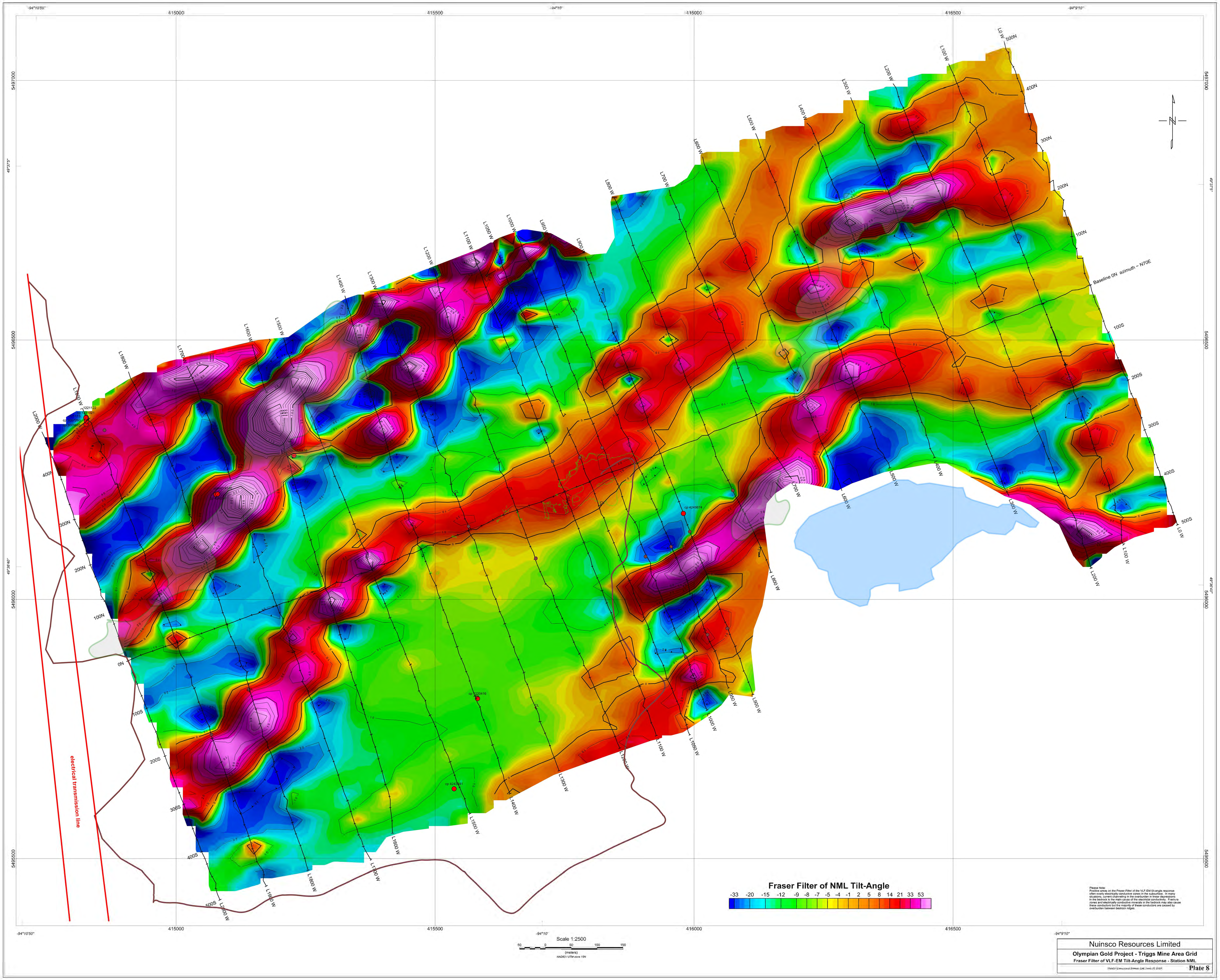
415000
415500
416000
416500
5497000
5496500
5496000
5495500
Baseline 0N azimuth = N70E
electrical transmission line
Fraser Filter of NML Tilt-Angle
-33 -20 -15 -12 -9 -8 -7 -5 -4 -1 2 5 8 14 21 33 53
Scale 1:2500
(meters)
Please Note:
Positive areas on the Fraser Filter of the VLF-EM tilt-angle response often overly electrically conductive zones in the subsurface. In many situations, current channeling in the overburden in linear depressions in the bedrock is the main cause of the electricial conductivity. Fracture zones and electrically conductive minerals in the bedrock may also cause these conductors but the majority of these conductors are caused by overburden between bedrock ridges.
Nuinsco Resources Limited
Olympian Gold Project - Triggs Mine Area Grid
Fraser Filter of VLF-EM Tilt-Angle Response - Station NML
Plate 8

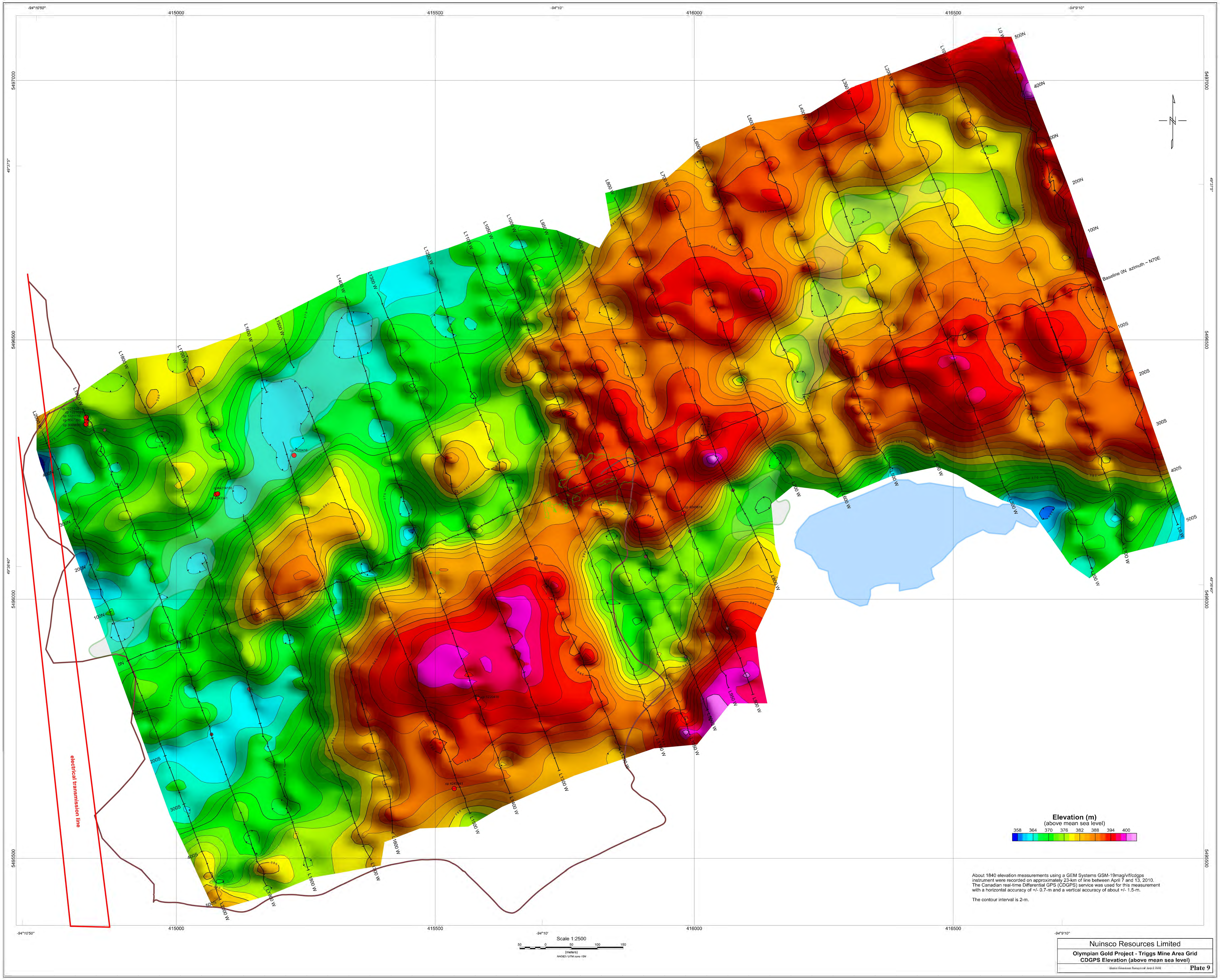

415000
415500
416000
416500
5497000
5496500
5496000
5495500
Baseline 0N azimuth = N70E
electrical transmission line
Scale 1:2500
(meters)
Elevation (m)
(above mean sea level)
358 364 370 376 382 388 394 400
About 1840 elevation measurements using a GEM Systems GSM-19mag/vlf/cdgps instrument were recorded on approximately 23-km of line between April 7 and 13, 2010. The Canadian real-time Differential GPS (CDGPS) service was used for this measurement with a horizontal accuracy of +/- 0.7-m and a vertical accuracy of about +/- 1.5-m.
The contour interval is 2-m.
Nuinsco Resources Limited
Olympian Gold Project - Triggs Mine Area Grid
CDGPS Elevation (above mean sea level)
Plate 9